LA-UR-25-30467

Approved for public release; distribution is unlimited.

Title:	Real Time, In-line Monitoring of Hanford Tank Wastes - Year 1 Report
Author(s):	Lakis, Rollin Evan; Smith, Nicholas Alexander; Pantea, Cristian; Junghans, Ann Sylvia; Piper, Jacob Martin; Kurtz, Eli Samuel Rowan; Cockram, Ezra Faith; Lascola, Robert; Tadzik, Shawnna; Howe, Anthony; Grover, Martha; Crouse, Steven; McDaniel, Dwayne
Intended for:	Report
Issued:	2025-10-22

Los Alamos
NATIONAL LABORATORY

Los Alamos National Laboratory, an affirmative action/equal opportunity employer, is operated by Triad National Security, LLC for the National Nuclear Security Administration of U.S. Department of Energy under contract 89233218CNA000001. By approving this article, the publisher recognizes that the U.S. Government retains nonexclusive, royalty-free license to publish or reproduce the published form of this contribution, or to allow others to do so, for U.S. Government purposes. Los Alamos National Laboratory requests that the publisher identify this article as work performed under the auspices of the U.S. Department of Energy. Los Alamos National Laboratory strongly supports academic freedom and a researcher's right to publish; as an institution, however, the Laboratory does not endorse the viewpoint of a publication or guarantee its technical correctness.

Real Time, In-line Monitoring of Hanford Tank Wastes

Year 1 Report

LANL

Rollin Lakis, Nicholas Smith, Cristian Pantea, Ann Junghans, Jacob Piper, Eli Kurtz, Ezra Cockram

SRNL

Robert Lascola, Shawnna Tadzik, Anthony Howe

Georgia Institute of Technology

Matha Grover, Steven Crouse

Florida International University

Dwayne McDaniel

LA-UR: 25-30467

Table of Contents

Introduction

The team comprised of students, postdocs, early, mid and senior career scientists from Los Alamos National Laboratory, Savanah River National Laboratory, Georgia Tech and Florida International University, with the guidance of H2C, is developing a suite of in-line instruments for the Hanford high level waste (HLW) and low active waste (LAW) processes to provide near-real-time analysis of waste-form physical properties and composition. The work builds on results from the recent DOE-ORP, EM Technology Development and other projects that demonstrated promise for the use of real-time in-line monitoring (RTIM) to measure chemical compositions of slurries of up to 20 weight % solids. The goal is for this instrument suite is to substantially reduce the need for sampling for process control. Sample waste, exposure associated with sample analysis, and the demand for an external laboratory facility would be greatly reduced. The throughput of waste treatment systems would be improved by elimination of the downtime caused by waiting for sample results. This translates into reduced process storage as process knowledge will be continuously updated in near-real-time. These breakthrough technologies would significantly reduce the life cycle cost and accelerate the schedule for the Hanford tank waste mission.

The advanced elemental, molecular and physical characterization methods employed are adopted from industry and academic research and adapted in a manner that yields significant efficiency and quality dividends for the operator. Elemental analysis by laser induced breakdown spectroscopy (LIBS) is being improved to permit flexible and efficient sampling of diverse process streams with new methods that enhance detection sensitivity. New approaches to attenuated total reflection-Fourier transform infrared spectroscopy (ATR- FTIR) and Raman spectroscopy will provide enhanced molecular characterization of slurry systems. Instruments and methods are also being developed to make physical property measurements directed at the characterization of slurries in pipes and tanks. These developments will leverage advanced concepts for in-line rheology and physical acoustics to characterize the properties of slurries in motion. These methods may be relatively easy to implement in complex environments and could be very important when slurry measurements may suffice as a surrogate for more complex elemental and molecular characterization. Data integration methods and advanced data analysis will be explored to achieve the maximum possible information from diverse analytical methods and data streams. This effort will also consider an evaluation of historical Waste Acceptance Criteria (WAC) data to understand relationships between analytes and properties and rigorously develop a suitably reduced suite of properties to target. This will provide the greatest range of technological options for implementations required in a highly constrained environment.

This work is being conducted on a common set of slurry simulants that subsequently will span a representative range of chemical and physical properties. The results from analyses of this baseline set will help establish the correlations between the methods. Radiological facilities at the National Laboratory partners will be included to evaluate the effects of exposure on the instrumentation. In the last year of the work, the technologies will be brought together at a non-radiological pilot-scale facility to test and demonstrate their use in a sampling environment that is otherwise similar to what is available at Hanford.

Once developed and proven in their specific application, we anticipate that the approach can be easily adapted to different sets of materials and/or facilities, expanding the potential use cases way beyond LAW and HLW process at Hanford.

Year 1 Programmatic Summary

The project team is generally on track with all proposed research, purchases, and milestones/deliverables. This report will address the details of the different research areas below. In general, the first year of this project was dedicated to understanding the waste stream and how the proposed technologies can measure those streams in a laboratory environment. This is the first step to understanding how the technologies can be deployed in the field at the Hanford site. Several conversations were held between the project and contacts in H2C responsible for the waste campaigns that will be sent to direct feed low active waste (DFLAW). These interactions provided the project with valuable information on waste composition and physical properties, as detailed in the waste form simulate section below, and started the pre-engineering conversations to understand how the project could potentially interface these technologies with the larger Hanford tank system. Fundamentally, each component of the project started to develop concepts to ensure that their technologies could perform their stated goals, elemental or chemical composition or rheological measurements, in the associated waste streams in the described waste transfer systems. For all components of this project, the first mission is to understand the responses of the analytical instruments to progressively more complex samples. This allows the project to understand the signals caused by the increase in complexity and build sequential increases in knowledge.

Project Year 1 was marked by a number of large equipment purchases for all of the individual project components. This included critical equipment that was needed to carry out the scientific mission in the first year and beyond. Due to the need to procure several long lead items, a slower research pace was observed in the first year. Despite some additional purchases in project year 2, an increased pace of research is expected.

This report will detail the various major “thrusts” of this project. The first of these is elemental and chemical characterization of the waste stream. Specifically, the techniques are looking for elements such as aluminum, iron, potassium, sodium, zirconium, and sulfur and chemical species such as nitrates, nitrites, sulfates and other associated forms in a high pH environment. The concentration of these species is a vital metric in order to meet waste acceptance criteria and to ensure that produced glass wasteforms are suitable for long term storage and disposal. The specific technologies under investigation are Laser Induced Breakdown spectroscopy (LIBS), Attenuated Total Reflectance Fourier Transform Infrared spectroscopy (ATR-FTIR), and Raman spectroscopy.

The second thrust of this project is to understand the physical and rheological properties of the waste streams. This includes studying the rheology of the flowing systems and understanding physical properties via as pressure drop methods, shear stress measurements, and frequency domain acoustic properties. The goal of this thrust is to understand the physical composition of the waste streams, how they are transported, and what their critical parameters for transfer between tanks and to processing mechanisms, including the solid loading factor. This is a critical component of the elemental and chemical characterization for species that exist in multiple phases (Na, Al, Ca, etc.). Therefore,

understanding the exact solids loading independent of the elemental and chemical characterization is important for a complete workup of any flowing waste stream. In addition, this thrust is tasked with designing and building a test loop that will present a flowing slurry with representative solids loading and at speeds expected at the Hanford tank farm. Based on discussions with our partners we expect these speeds to be in excess of eight feet per second. Techniques under investigation are in-line pressure drop, flow rate, and density measurements for yield stress determination.

The third thrust in this project involves the study and creation of waste form stimulants. While the variability of chemistry present in the Hanford tanks is extraordinary, a representative slurry sample must be created for inter-comparability between methodologies. To do this teams examined historical data from the tank farms, looked for correlations and commonalities across multiple series, and then created a procedure for creating simulant waste streams with appropriate characteristics.

Finally, the fourth thrust of this project is to incorporate data fusion and data science techniques to combine information from the disparate analytical techniques. This fusing of information from multiple complementary techniques is expected to allow the project to predict and understand the elemental and chemical composition up of the solutions as well as their physical characteristics. It will allow for off normal event monitoring and trends in online data to be presented in a way that can be easily digested. However, this is the least defined aspect of the project as data fusion synergies are typically only found mid project when there are large enough data sets generated. A priori, we are unable to provide more than hypotheses of what data streams will be compatible and synergistic.

Elemental/Chemical Characterization

There are two separate areas of experimental work in the elemental chemical characterization. One of them is the use of laser induced breakdown spectroscopy to determine elemental concentrations. This is supplemented using ATR-FTIR and Raman spectroscopy dip probes to study the chemistry of the waste systems. The development of these individual pieces will be described below with focus on the experimental setup and design of the systems as well as how they're interfacing with the similar slurries used in the first year of this project.

LIBS

LIBS: Sampling Method Development - Falling jet setup

The analysis of liquids using LIBS has previously been shown to be improved by surface enhancement techniques, including what is known as the falling jet (or laminar jet) method. By forming a flowing liquid into a laminar stream, signal is enhanced, and noise is reduced; the uniform surface of the liquid allows the laser to uniformly ablate the material and improves coupling, and the stability of the jet ensures that the correct focal depth is preserved across measurements. This approach may be directly applicable to the Hanford mission if a suitable slipstream can be generated on a waste line. More importantly, the technique serves as a method to improve the quality of LIBS measurements in the laboratory to understand solution and slurry behaviors. Measurements of solution phase constituents are relatively simple but more complex than solids samples (metals, ceramics, etc.); creation of slurries to allow for sampling of the solids and solutions in a reproducible fashion is a significantly more complex problem. As DFLAW is pumped from the underground tanks, our goal is to be positioned to be able to have a

workable sampling method, e.g., drawing a slipstream from this high velocity flowing slurry and applying the LIBS analysis to this portion of the waste. To support this goal, we have been performing experiments designed to showcase the effectiveness of the falling jet method as applied to waste simulants.

Initial steps have included the design of laminar flow nozzles and the assembly of a slurry testing platform directly on laser tables. In this apparatus, a lower receptacle continuously stirs the slurry to keep particles suspended in solution, while a pump delivers this slurry to an upper hopper. The solution is gravity fed through the nozzle and subsequently passed through the focal point of the LIBS laser and then returned to the lower tank. While this solution is only applicable to bench-scale experiments, it is meant to be a proving ground that will allow us to measure waste simulants without generating large quantities of contaminated waste and understand the spectral qualities of the materials.

To date, we have conducted measurements primarily focused on detection of lower hazard materials such as Ca, Na, and Cl in both dissolved (e.g., $CaCl_2$) and slurried forms (e.g., water mixed with insoluble Wollastonite powder, $CaSiO_3$). To date, reliable analysis of slurries has been a challenge and high variability has been a primary concern. Figure 1 shows initial CAD drawings of sample delivery systems. The use of 3D printers has allowed for rapid, even daily, prototyping to move us closer to a reliable sample delivery system. A successful setup and the spectra obtained from interrogating the flowing liquid with LIBS is shown in Figure 2.

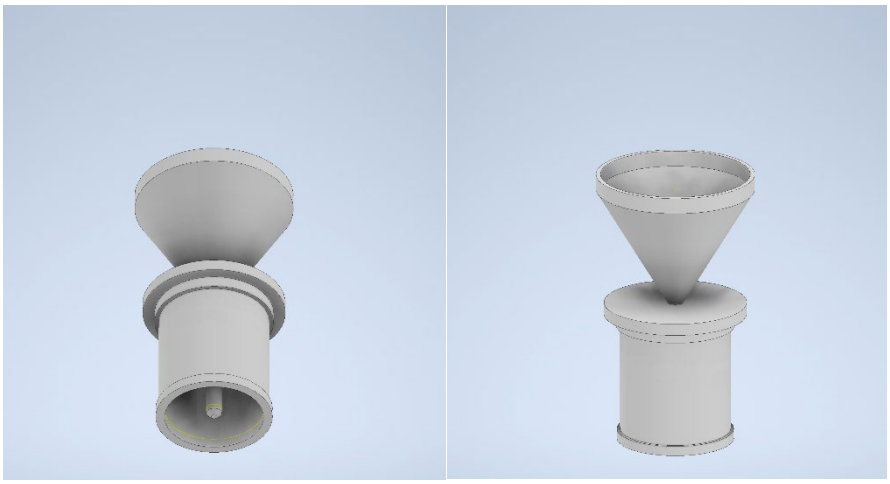

Figure 1 - CAD drawings of a laminar flow nozzle, allowing stirred slurries to be formed into uniform streams.

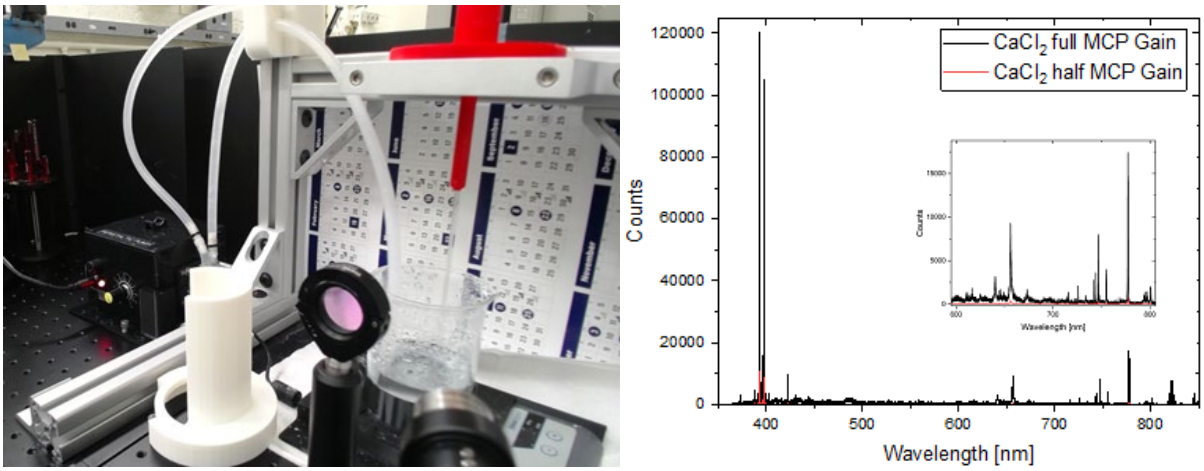

Figure 2 - Setup of continuous flow sampling (left) and spectra, demonstrating successful in-line or at-line implementation for near real time process control and verification. (Experimental parameter for spectra: 350 mL/min flow, 10 g CaCl2 in 200 mL H2O, 10 shots averaged)

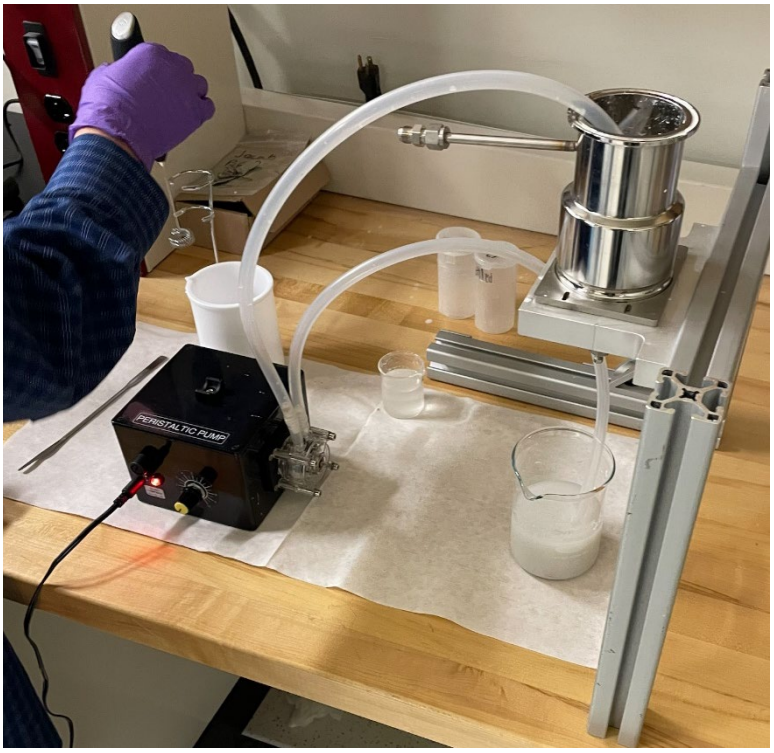

Figure 3 - Initial work to create laminar flows with slurried samples (wollastonite).

LIBS: Equipment Design & Calibration

Major goals for the first year of this project were to design and implement the loop system based on existing and new equipment. The existing OnSpec laser system was utilized as much as possible to start experiments on varying types of dissolved and slurried chemicals. This was further augmented with the delivery of a tabletop laser system from Lumibird, the Q-Smart Twins system, a double pulse LIBS system, shown in Figure 4. This was coupled with an Aryelle echelle spectrometer (LTB, Germany). This system was used for initial single pulse determinations of solutions and slurries. As the behavior of the

waste streams needed to be studied under single pulse LIBS conditions first, the system was utilized in that manner. The double pulse capability will be more fully utilized in year 2 when a LIBS controller will be delivered during project year 2 to allow for the fine interpulse timing requirements of double plus LIBS. Double pulse LIBS is expected to increase analyte signal and produce more reliable data.

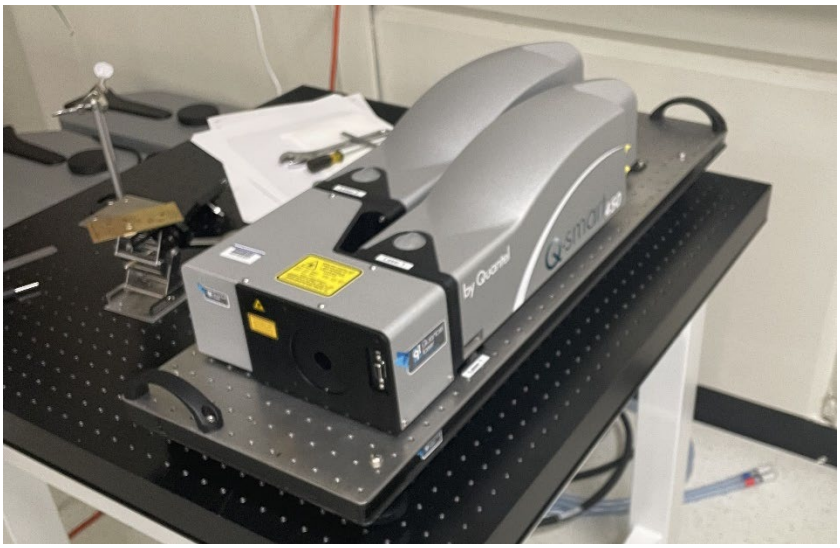

Figure 4 - Lumibird Q-Smart Twins system.

The echelle spectrometer (Figure 5) is configured to collect plasma signal light via fiber optics using COTS optical components. The system is calibrated using a manufacturer provided calibration light source; the spectrometer control software automatically calculates corrections and pixel shifts to ensure that the collected light has an accurate wavelength calibration. This has aided in our ability to assign transitions to particular elements especially in noisy regions where there are multiple potential assignments and wavelength accuracy is key.

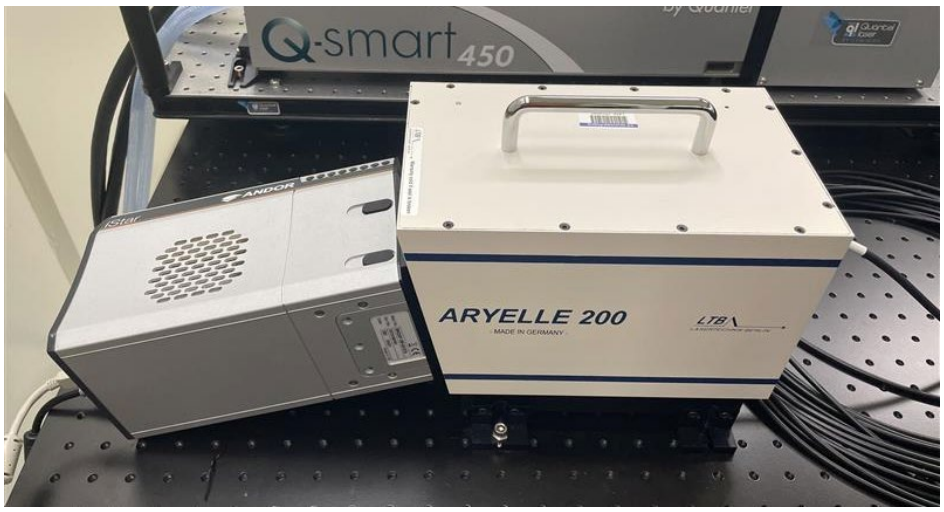

Figure 5 - LTB Aryelle 200 Eschelle spectrometer.

LIBS: Method Development & testing

A significant amount of effort was devoted to developing an analytical method for the measurement of solution and slurry samples. The method development has centered around the interface between the sample matrix and the laser and the optimal Digital Delay Generator settings (such as delay time, integration time, intensification, etc.), which needs to be optimized for each system configuration.

The most challenging aspect of the first year of work was finding methods to present a reproducible surface for sampling both liquid and slurried samples. Several off-the-shelf techniques exist for sampling solutions but there are few examples in the literature or in commercial space on producing a reproducible sample with a slurry feedstock. A system optimization needed to be performed for every iteration of the system, requiring some re-work and re-measurement of samples as the system improved. Some spectra from the first year are show below (Figure 6 – Figure 9, below) that demonstrate the system performance checks and samples measured during the first project year.

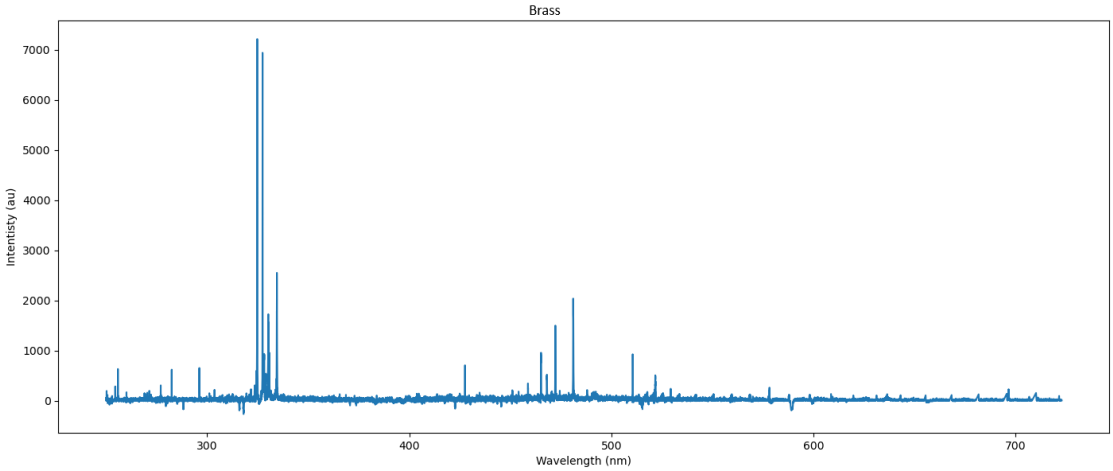

Figure 6 - Calibration spectrum of Brass coupon. Prominent Copper and Zinc lines are observed at 324 nm, 327nm, and 521nm and 468 nm, I 472 nm, and 481 nm respectively.

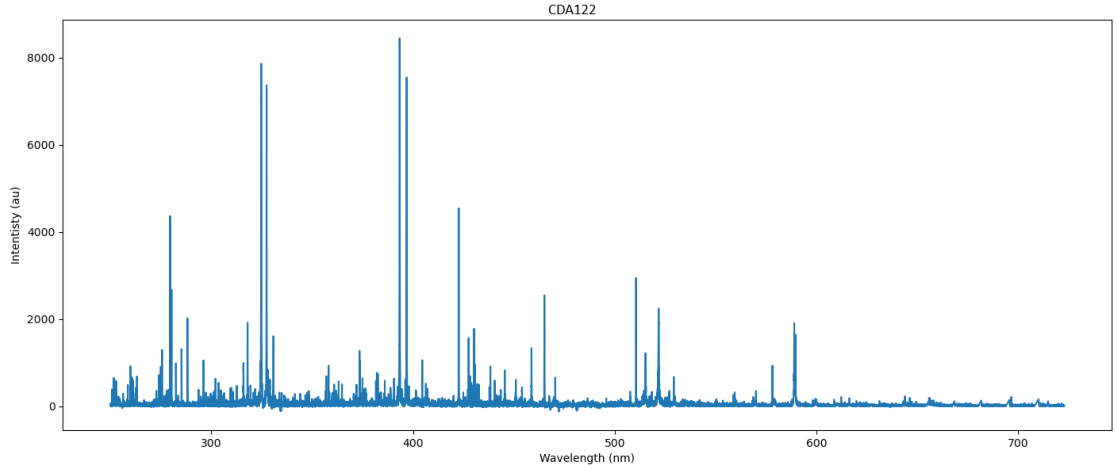

Figure 7 - Calibration spectrum of Copper alloy CDA122. Copper lines can be observed at 324 nm, 327nm,and 521nm while minor contributions from calcium can be observed at 393 nm, 396 nm, and 589 nm, and sodium at 589 nm.

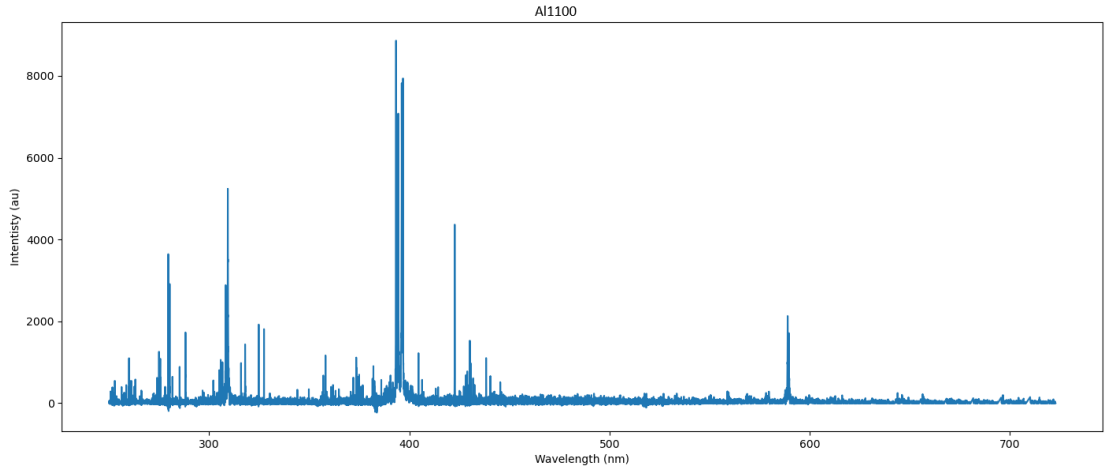

Figure 8 - Calibration spectrum of Aluminum alloy AL1100. Aluminum peaks can be observed at 394nm and 396 nm

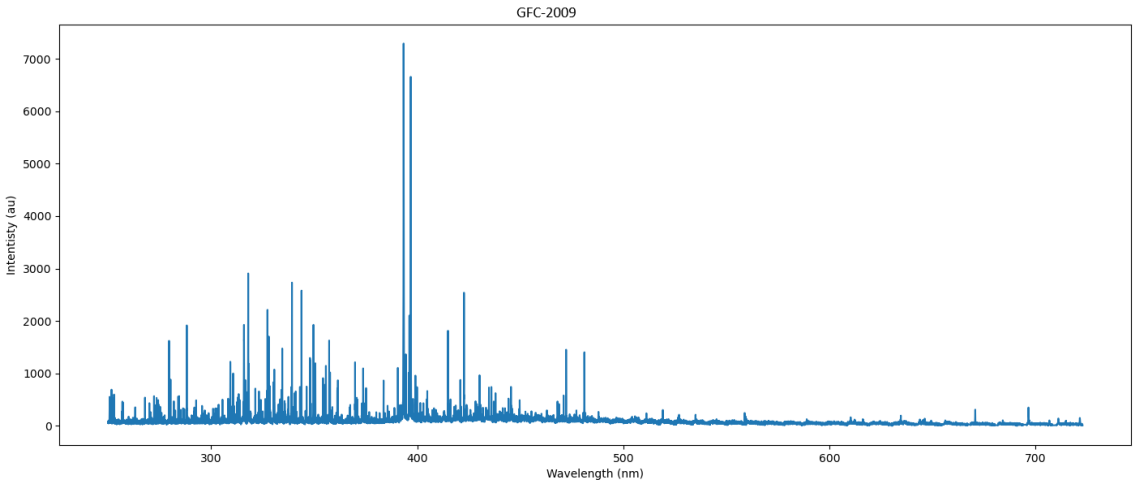

Figure 9 - Spectrum of dry sample of Glass Forming Composition 2009 composed primarily of Si, Al, Fe, Zn, Zr, Mg, and Ti. The prominent Aluminum lines can be observed at 394 nm and 396 nm.

Scoping study: LIBS induced acoustic shock waves

To support characterization of tank waste and vitrification efforts at the Hanford waste site, we are also evaluating acoustic signals from LIBS plasma formations for their use in differentiating material properties. This is based on the fact that in LIBS, a pulsed laser source energizes and ablates a target material, resulting in the formation of a weakly ionized plasma containing vaporized target species. The near instantaneous liberation of energy through the plasma's initial expansion induces the formation of a strong shock wave. The shock wave inevitably decays, leaving an acoustic wave that can be recorded with a microphone.

For the initial work, we used a commercial SciAps Z300 handheld LIBS analyzer and Behringer ECM8000 microphones, and recorded LIBS plasma formations on a series of metal coupons and porous glass disks. We then examined features of the waveforms including peak amplitude and total energy of the wave. We analyzed these features to determine their usefulness in differentiating between materials using LIBS-acoustic signals.

Figure 10 - Condenser microphone used to measure acoustic waveforms from the LIBS plasma formation.

The main metric we aimed to collect was the acoustic energy of the wave at a fixed distance away from the plasma. Acoustic energy is related to the deposition energy of the laser, the plasma formation, and also potentially influenced by the substrate material properties. By fixing the microphone at a set distance, the differences observed in the peak pressure / integrated energy can be inferred to be caused by the energetic difference between the plasma generation events, e.g. a more energetic wave recorded at 10 cm from the plasma indicates a more energetic plasma formation event, which we hypothesize can be used for differentiating material properties.

Analysis of the acoustics generated on the CDA (copper alloy) and aluminum coupons showed well defined and consistent responses from the materials; however, significant differences between the coupons were not observed in the initial N-wave we are interested in. Figure 11 displays the acoustic responses from each coupon.

We also measured 3 glass disks of different porosities (25-50, 70-100, or 145-174 micron pore diameter). Materials produced well defined wave forms that were able to be recorded consistently. Differences were more pronounced than for the Al and CDA coupons, but still for the most part not significantly different from each other in the initial N-Wave.

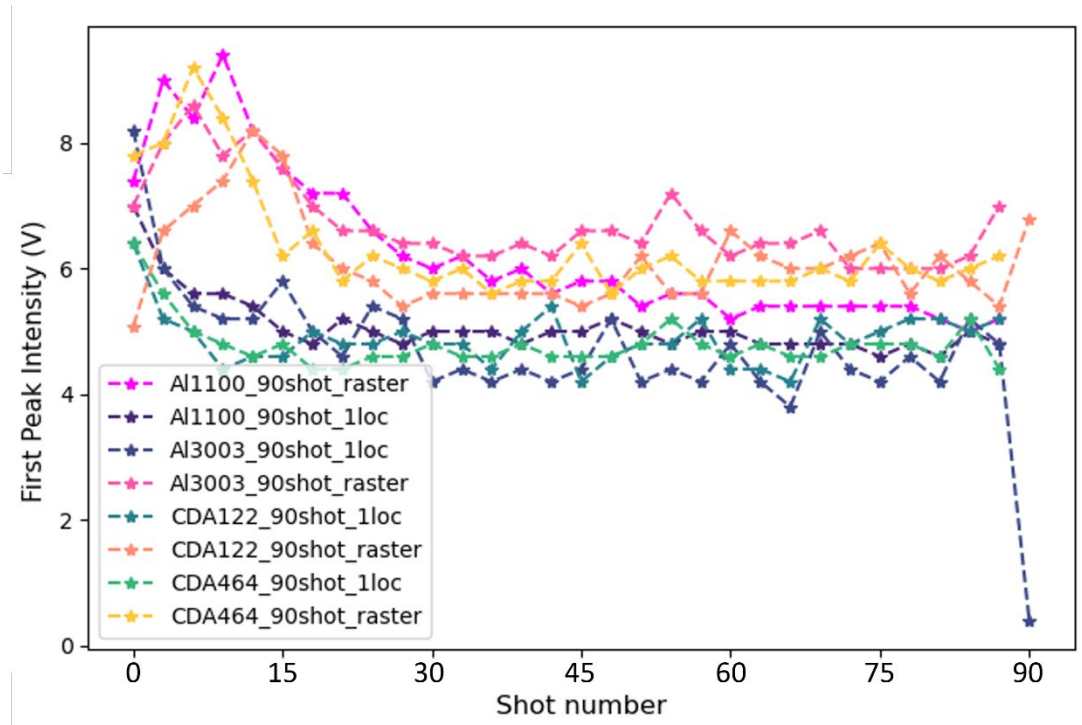

Figure 11 - Acoustic signals from various metal coupons. The figure shows the evolution of peak acoustic intensity over subsequent laser shots, in both raster and single-location mode.

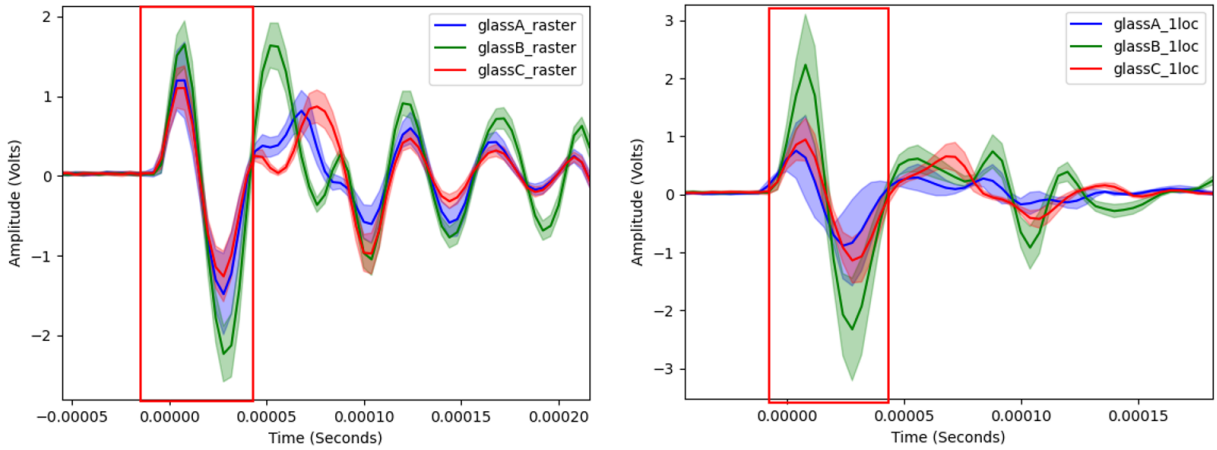

Figure 12 - Acoustic signals from porous glass disks. Color shading indicated 1 Standard Error. Red bounding boxes indicate regions of interest.

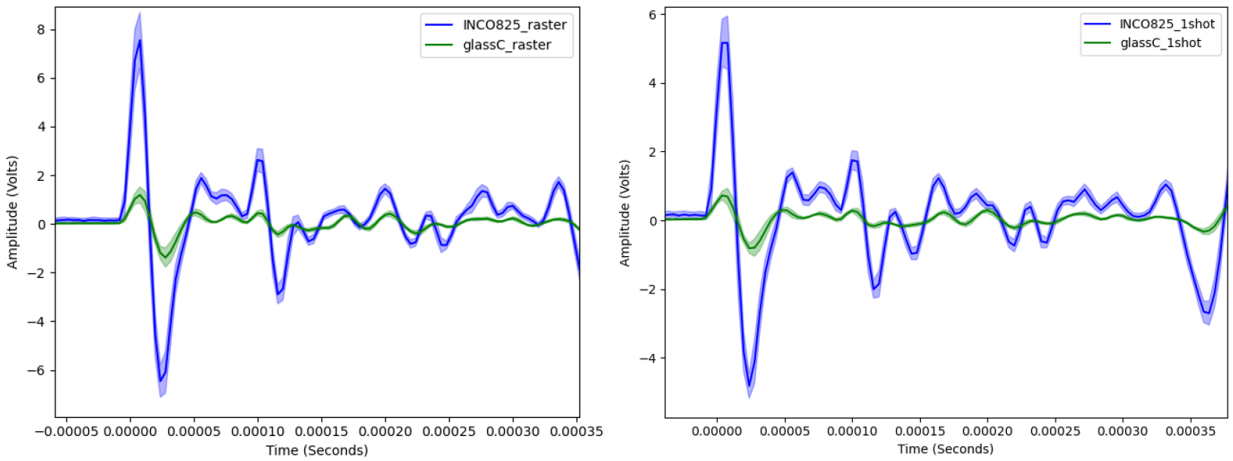

Figure 13 - Acoustic signals from glass C and INCO coupon in raster and single location mode. Color shading indicates 1 Standard Error.

While it is difficult to discern significant differences between the glass disks based on the acoustics, it is clear that acoustics can help differentiate between the glass disks and metal coupons. The difference in amplitude and integrated energy of the first waveform is obviously very significant when observed between glass C, the densest glass, and a metal coupon.

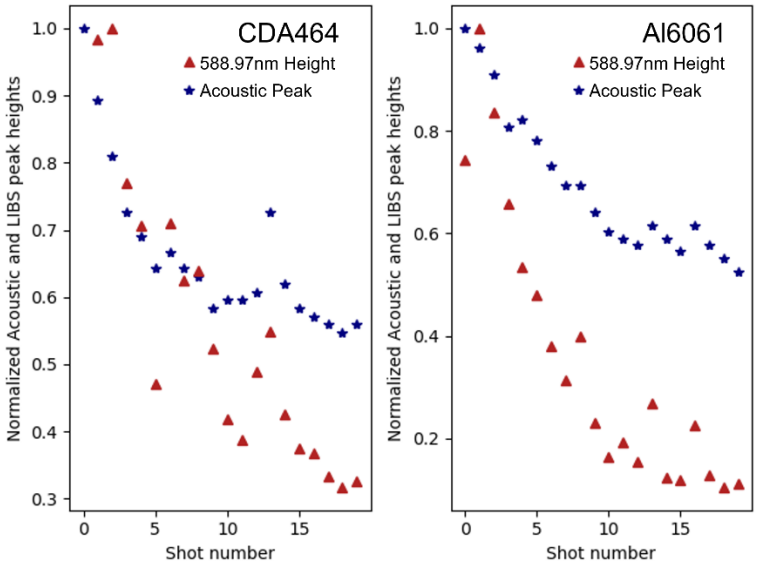

Figure 14 - Displays the relationship between acoustic and spectral line intensity for both CDA464 and Al6061

Additionally, we performed a series of spectral measurements and collected associated acoustic responses from each measurement. This was done to see how well the intensity of an acoustic signal was correlated with the intensity of the LIBS spectral lines. This relationship is explored and both acoustic peak height and the spectral peak height of Na located at 588.97 nm decrease over successive shots. (Figure 14) Generally, the idea that a louder acoustic signal indicates stronger emissions is excepted, however, the exact nature of the relationship and the predictive nature of one variable on another is as yet unexplored. We will continue to pursue this research, with the ultimate goal is to use

the acoustic peak pressure as a normalization factor across successive shots for their spectral content, or to use the acoustic energy as a fast “dud” checker, to quickly exclude shots that do not couple well to the substrate.

The low laser power of the Z300 handheld LIBS instrument prevented us from obtaining acoustic measurements of LIBS performed on liquid media. It also may have affected the signals gained from solids, such as the porous disks. We are currently repeating this work with our Twin Laser system and will also introduce different materials, such as slurries, powders, and solids with different densities. For slurries of different densities, we expect to utilize the acoustic response of LIBS plasmas to analyze the density of the slurry. We also anticipate that with repeated shots at a flowing slurry, we may be able to construct a weighting factor with which to augment the spectral components of each shot based on their acoustic response, in order to achieve a more accurate picture of the average slurry density / content.

ATR-FTIR and Raman Spectroscopy

Attenuated total reflectance – Fourier transform infrared (ATR-FTIR) spectroscopy has historically been used to monitor the solution phase of slurries in real-time and remotely. Therefore, the technology is a fitting candidate to measure the concentration of dissolved anions in nuclear waste. However, nuclear-waste presents hurdles that may make data acquisition with ATR-FTIR spectroscopy difficult: nuclear-waste is radioactive, highly multicomponent, and may foul probes. For a discussion of ATR-FTIR probe resilience under radioactive conditions, see the Probe Irradiation section below. The present section focuses on results that have bearing to multicomponent monitoring in the presence of probe fouling.

Molecular quantification of soluble anions was sought with spectroscopy in slurries typical of nuclear waste. While building quantification models for ATR-FTIR spectra, fouling was observed on the ATR-FTIR probe tip (diamond in a concave configuration). Subsequent analysis revealed that the fouling matched literature references for gibbsite, $Al(OH)_3$, which was a significant component of the slurries being measured. The intensity of the fouling signature can be seen to increase over time in Figure 15. The fouling was removed via computational methods including two blind source separation (BSS) methods and nonnegatively constrained classical least squares (NCCLS). Figure 16 shows that using NCCLS improved quantification with ATR-FTIR spectra in slurries typical of high-level waste. Notably, it is shown that the ATR-FTIR probe can accurately quantify soluble species (i.e. nitrate, nitrite, and sulfate anions) expected in slurries typical of high-level waste. Additionally, this study revealed that using wt.% of the *solution phase* (rather than the entire slurry) significantly improved the accuracy of ATR-FTIR predictions; ATR-FTIR spectroscopy cannot effectively measure insoluble solids suspended in a slurry and so insoluble solids should not be included in the calibration procedure.

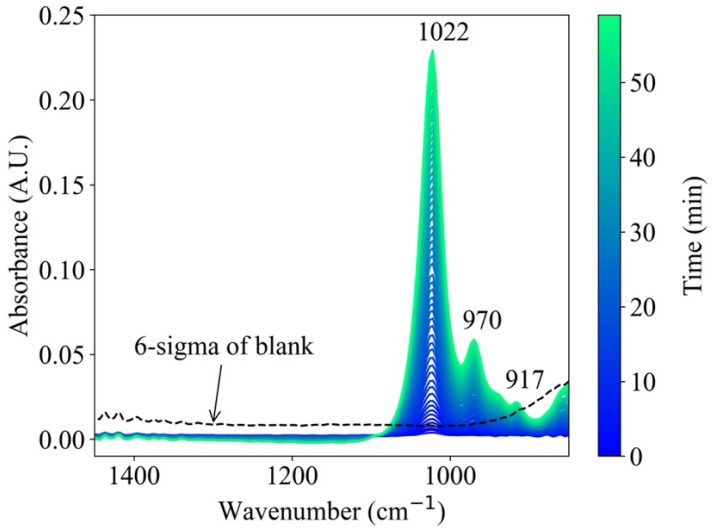

Figure 15 - Gibbsite fouling in the ATR-FTIR spectrum as a function of time (minutes) since the introduction of gibbsite. The dashed black line indicates six standard deviations of 40 "blank" spectra consisting of 100.00 g H2O and 12.02 g NaOH. The spectra shown are measured from the same solution with 0.0247 g undissolved gibbsite ($Al(OH)_3$) added and suspended via a stirrer at 400 rpm.

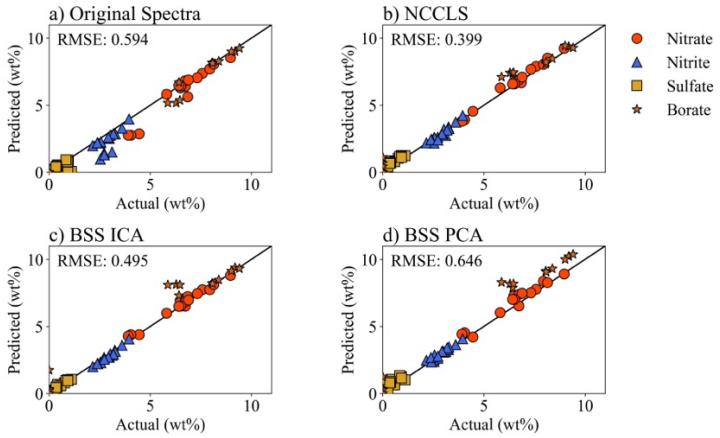

Figure 16 - Quantification of four soluble anions in slurries using a partial least squares regression model with a) no preprocessing. Additionally shown are plots of quantification with computational removal of the gibbsite fouling provided by b) nonnegatively constrained classical least squares, c) blind source separation with independent component analysis, and d) blind source separation with principal component analysis[i].

Probe irradiation

Recent work has established that probe-based optical spectroscopy techniques such as Raman or attenuated total reflectance (ATR) – Fourier transform infrared (FTIR) spectroscopy are promising candidates for the *in situ* or at-line chemical analysis of slurries.[ii] Slurries present numerous challenges for any material in contact with or in proximity to them. For example, solids deposition on a probe window has been observed on prolonged exposure of Raman probes to slurry simulants with silica solids.[ii] The solids, if left unaddressed, would eventually block the transmission of light to the sample. Solids flowing at high speed could also scratch probe windows, reducing transmission, if hard materials such as sapphire are not chosen.

Another challenge to RTIM measurements of HLW slurries is the effect of radiological exposure on the probes. In general, optical fibers and windows have been observed to be tolerant of radiation exposure[iii], especially for materials with high-OH content, and have been used for extended periods of time in radiological processing facilities and hot cells. Raman probes with these elements rely on the transmission of light. Any window or fiber darkening upon radiological exposure can be compensated with a periodic re-referencing of the baseline transmission properties of the material, and if necessary, can also be reannealed at elevated temperatures. Otherwise, the basic properties of the measurement, such as the effective sampling volume of the Raman excitation, remain the same.

The principle of ATR measurements differs from Raman or regular absorbance measurements in ways that admit new possibilities for radiological impact on measurement performance. The light beam in an ATR probe bounces off the underside of the probe window according to the principle of total internal reflection (Figure 17). The interaction of the light with the sample is entirely due to the presence of an evanescent wave that exists on the outside of the probe window. This wave, exponentially decaying in intensity as a function of distance from the window, allows for a measurement that is specifically sampling a very short distance (~ 1-10 microns) into the surrounding medium. If that light is absorbed by the solution, the intensity of the internally scattered light will be measurably affected.

As shown in Figure 17, the effective penetration depth d_p depends on the angle of interaction of the light with the exterior surface. In benign circumstances, that angle is fixed due to stability of the internal optical alignment of the probe and the surface of the ATR window. However, it is conceivable that the distribution of angles experienced by the light beam during reflection will be broader due to radiation-induced surface roughening. This would change the effective penetration depth, leading to a change in the absorbance of the evanescent wave. The literature on the effect of beta or gamma irradiation on the surface properties of materials (such as poly-crystalline diamond) commonly used in ATR measurements is not extensive. Therefore, we have decided to explicitly assess the potential effect by irradiating an ATR-FTIR probe and observing the effect, if any, of the radiation on measurements of a chemical sample.

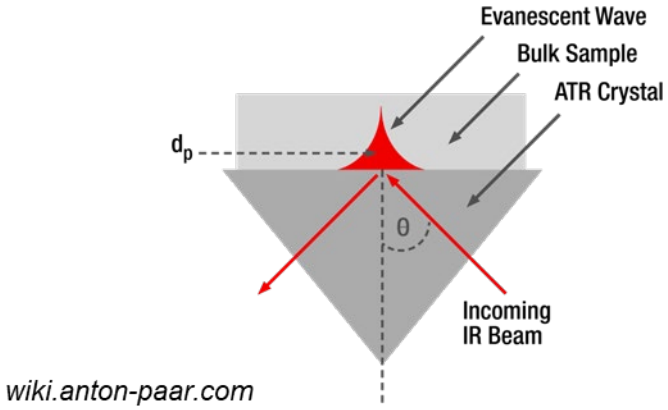

$$d_p = \lambda / 2\pi n_1 (\sin^2\theta - (n_2/n_1)^2)^{1/2}$$

Figure 17 - Schematic of ATR configuration and formula for the depth of light penetration (d_p) as a function of angle of incidence θ.

Methods

The ATR probe used in the testing is the Mettler Toledo DST DiComp direct injection probe (Figure 18). Probe parts that would be in contact with the slurry are: the probe body, which is constructed of C-22 Hastelloy; a gold seal between the body and window; and, a window made of polycrystalline synthetic diamond. A new probe was purchased for these tests. The DiComp probe is designed for use with the Mettler Toledo ReactIR Fourier transform infrared spectrometer; such an instrument already owned by SRNL was used for assessment of the probe's performance after doses of radiation, as described below.

Figure 18 - DiComp ATR-FTIR probe.

Irradiation took place at the Savannah River Site's Health Physics Instrument Calibration Laboratory using a nominal 50 milliCurie Strontium/Yttrium-90 source (beta irradiation). The solution-contacting end of the probe was positioned 30 cm away from the source. A jig was constructed to assure consistent replacement of the probe between dose steps. Cardboard shielding was implemented so that the end of the probe facing the radiation source was the only part of the probe exposed to the radiation. A dose program was designed so that the following cumulative doses would be delivered by the end of each step: 0.5 Gy, 1.0 Gy, 2.0 Gy, 3.0 Gy, 4.0 Gy, 5.0 Gy, 6.0 Gy, 7.0 Gy. Delivery of a 1 Gy dose required approximately 8 hours. After each dose, the probe was removed from the jig and taken to the ReactIR for evaluation.

Beta irradiation was chosen in order to concentrate the effects of the irradiation on the outer surface of the diamond window, where the evanescent wave effect occurs. In contrast, gamma irradiation would permeate the window, potentially impacting the other internal components of the probe and making it difficult to isolate the cause of any effect that was observed.

Standard diagnostic techniques available as part of the Mettler Toledo setup and spectral acquisition software were used to evaluate probe performance after each dose. After connection to the ReactIR, the probe position relative to the internal light source was auto aligned to maximize signal reaching the detector. This step reduced any potential variation associated with the probe removal. Two sets of diagnostic spectra were obtained. The first was a stability test, measuring four replicate transmission spectra with the probe tip in open air. The second was an acetone signal-to-noise test, with the probe immersed in research grade acetone, and absorbance spectra measured against an open-air reference. For the measurements taken after each dose, a new reference spectrum was acquired. This procedure removed any effects associated with lamp drift in the days/weeks between measurements.

Acetone and "blank" (open air) absorbance spectra taken before irradiation were used to create a simple partial-least squares (PLS) chemometric model, with acetone spectra assigned a concentration of 100% and open air a concentration of 0%. Although spectra were recorded over 650-2500 cm^{-1}, the data used in the model 1000-1800 cm^{-1} to include the primary acetone peaks at 1092, 1221, 1359, 1420, and 1767 cm^{-1}. These peaks correspond to the spectral region of highest output intensity of the ReactIR infrared source. Spectra were processed by taking the first derivative with respect to wavelength The PLS model required one principal component, as expected for a such a simple system. The prediction error for the initial (pre-irradiation) set was ±0.01% for the blank spectra and ±0.34% for the acetone spectra (1σ), providing a baseline assessment of probe and instrument performance.

Results and Discussion

By the end of Year 1 of the project, a total of 4 Gy had been applied to the probe. No changes to the probe were apparent to the naked eye. Repeated insertions of the probe into the ReactIR after each dose did not result in substantial intensity changes (the overall intensity decreased by less than 5% and the instrument passed internal tests). The acetone measurement test indicated a small (~2%) decrease in the predicted acetone value, with little change in the standard deviation of the replicates (0.34% pre-irradiation versus 0.31% after 4 Gy). The blank measurements and replicate standard deviation were consistent. The results are summarized in Figure 19.

The results indicate that the total dose applied to date does not substantially affect the probe performance. The probe remains functional and passes internal diagnostics. The small changes in the overall peak intensities could be compensated with periodic re-referencing. Given these observations, there is no indication that the window roughness has changed to a degree that would affect the penetration of the evanescent wave into the sample medium.

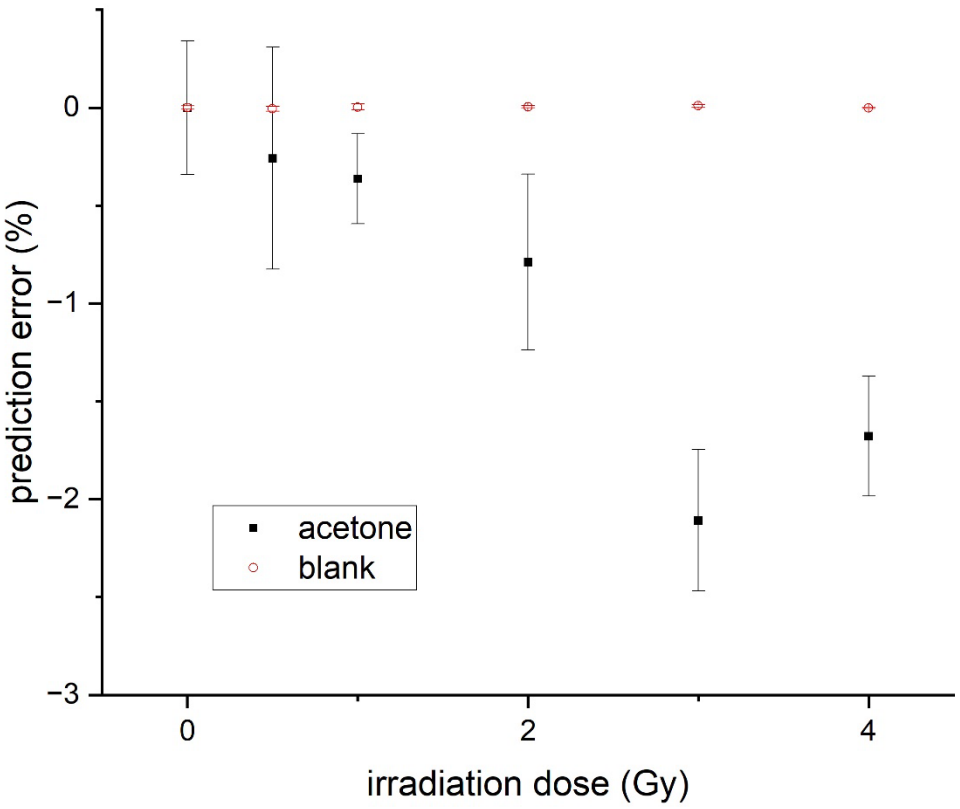

Figure 19 - Prediction errors for acetone diagnostic PLS model as a function of irradiation dose.

Future Work

Work in Year 2 will continue the dose plan until a cumulative dose of 7 Gy is reached, using the same spectroscopic performance diagnostics. Additional study will be performed using spare diamond windows procured from Mettler Toledo. These windows will be irradiated and observed using microscopic techniques in order to visualize any changes to the surface.

Data Fusion and General Data Science

Data management and data fusion are core principles of our monitoring approach moving forward. The complement of techniques investigated by this project will provide robust information about the whole slurry system that may inform real-time process decisions. To this end, we have begun by combining similar optical instruments available to our team: Raman spectroscopy, ATR-FTIR spectroscopy, and focused beam reflectance measurement (FBRM). Moving forward, the aforementioned optical instruments will be combined with LIBS to provide elemental analyses and acoustic measurements to interrogate density and rheological properties of waste in Years 2 and 3 of this project.

The three probe instruments discussed here combine to measure the molecular structure of both the solution (ATR-FTIR, Raman) and insoluble phase (Raman) of the slurry, as well as the chord-length distribution of suspended solid particles (FBRM). The data from Raman spectroscopy, ATR-FTIR spectroscopy, and FBRM, were combined via concatenation, scaled by mean-centering and dividing each feature by its standard deviation, and features of the combined data were extracted using principal component analysis. Using two traditional process monitoring techniques, Hotelling T^2 and squared prediction error, slurries were monitored for abnormal conditions.

Normal slurries were altered by introducing sensor failures, mixing changes, or unanticipated chemistry. With these varied faults appearing in the slurries, the aforementioned data fusion scheme outperformed any of the individual instruments for fault detection accuracy as shown by the confusion matrices in Figure 20, correct fault detection is indicated by data placed on the main diagonal (top left and bottom right) elements.. The decrease in correctly predicted normal conditions when fusing the data, compared to the ATR-FTIR and FBRM sensors alone, is caused by false positives predicted by Raman spectroscopy. This is investigated in the associated submitted publication and may be addressed through feature selection or richer training data.

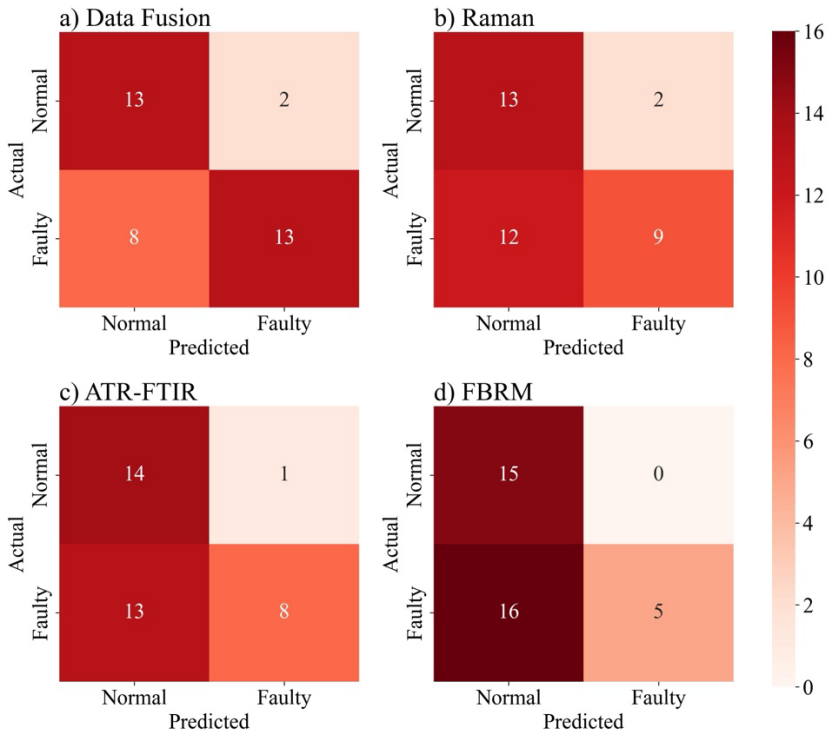

Figure 20 - Confusion matrices showing classes of predicted and actual faults in slurries typical of high-level nuclear waste. Shown are a) data fusion, b) Raman, c) ATR-FTIR, and d) FBRM schemes used for fault detection. The best methods will have the most data in the top left (correct normal prediction) and bottom right (correct faulty prediction) quadrants.

LIBS Numerical method development & Analytical results classification

LIBS is very powerful for rapid elemental analysis of materials in any physical state without much pre-processing, but in order to determine the relative concentrations of elements in an analyte, prior calibration curves, are necessary which can be time and resources consuming and/or hard to generate, especially for unexpected materials. Hence, we are looking into alternative ways to be able to assess the quality and quantity of materials investigated. In addition, we are also developing numerical methods that have the capacity to significantly enhance signal processing (e.g.,baseline and noise corrections) and element identification algorithms.

One point calibration

One-Point Multi-Line Calibration (OP – MLC) is an approach to only utilize one data point (versus usual 3 or more) and assumes that measurements are taken within Local Thermodynamic Equilibrium (LTE) and that the intensity is proportional to concentration. It is based on the concept of plotting intensity vs. intensity for multiple lines of the same element that allows the calculation of the correction factor, equal to the slope of the linear fit of these lines. (Figure 21)

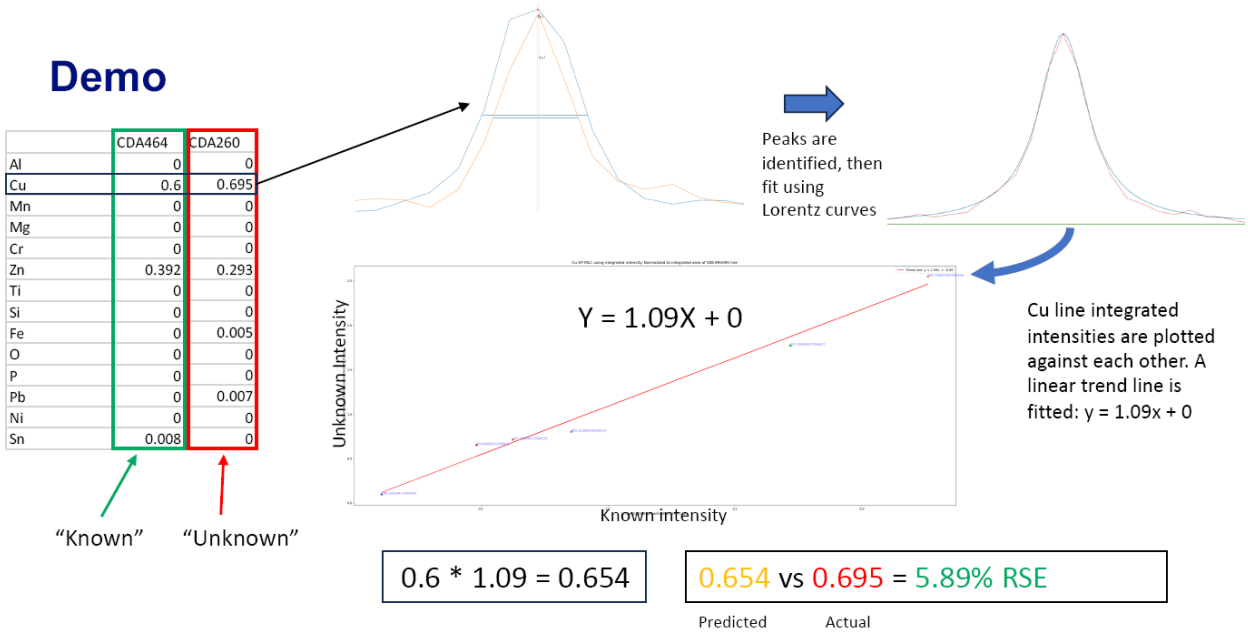

Figure 21 - Workflow of One-Point Multi-Line Calibration. Using only one elemental line is inaccurate. Using multiple lines generates a correction factor.

One advantage of OP-MLC is that it utilizes only one standard spectrum to calibrate an unknown sample and can be pretty accurate, especially if benefits are compared to the time/resource requirements. Drawbacks are that it requires the elements in the unknown sample to be present in the known standard, that it assumes LTE and homogenous conditions across shots as well as that it requires integrated intensity.

Software: Peak Analysis & Prediction

One other way to reduce the need for experimental pre-work necessary to be able to accurately identify and quantify materials investigated we investigate is to simulate different elements, combinations and ratios to help us identify spectra of unknown materials and/or ratios of materials.

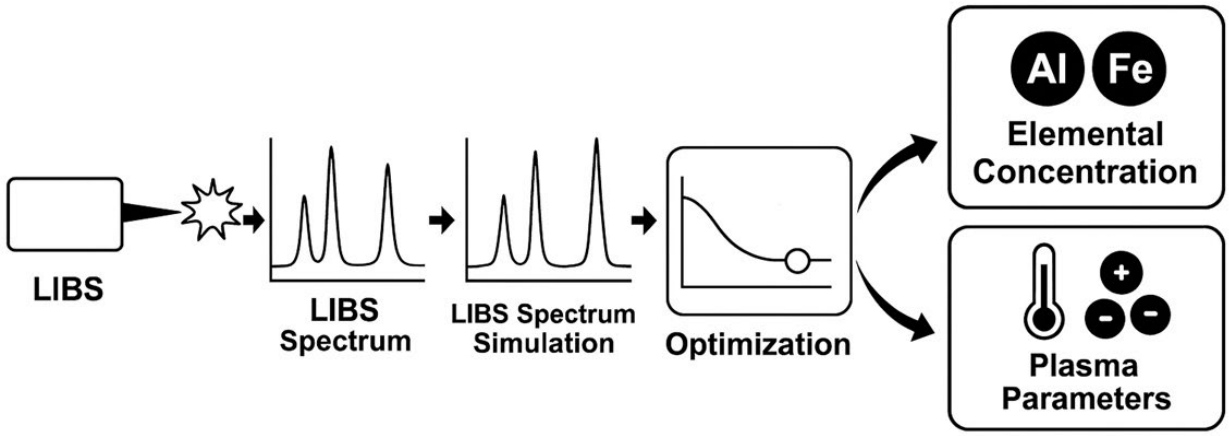

Figure 22 - Workflow of LIBS Spectrum Simulation. Elemental information as well as concentration, temperature, broadening and electron density is taken into account and relevant line information is collected and collated from the NIST database.

This could be especially useful when the expected concentration of materials is known – and hence can be simulated as a "standard", to be able to verify correct composition or flag potential anomalies quickly. (Figure 23)

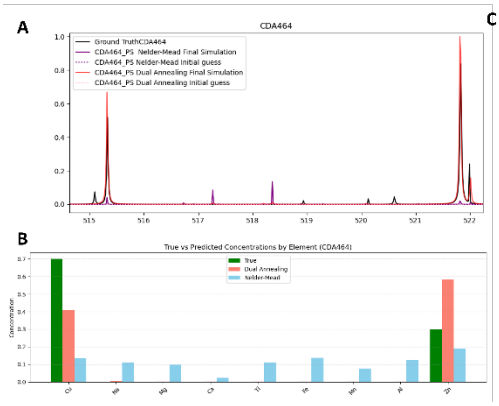

C

Sample	Element	True Conc.	Nelder-Mead	Dual Annealing	Calibration Curve
CDA706	Cu	0.89	0.134	0.934	0.747
CDA110	Cu	0.999	0.237	0.988	1.049
CDA122	Cu	0.999	0.228	0.983	1.046
CDA260	Cu	0.7	0.250	0.429	0.679
CDA360	Cu	0.615	0.257	0.339	0.621
CDA443	Cu	0.715	0.173	0.440	0.609
CDA464	Cu	0.7	0.134	0.410	0.691

Figure 23 - (A) Spectral simulation of a copper alloy, (B) Elemental concentration results of the simulation methods and (C) Comparison of the simulation results, shown along with the standard calibration method.

Physical and Rheological Properties

Noninvasive Acoustic Characterization

Acoustic Lab testing of acoustics techniques for acoustic properties determination will begin during the first project year. The relationships between sound speed, attenuation, density, and viscosity will be explored. Investigations into the identification of an appropriate multi-dimensional space for determination of concentration of solids in slurries. In addition, calibration curves for sound speed and perhaps density will be constructed for concentrations of interest in surrogate slurries.

Performed work:

This specific task, "Noninvasive Acoustic Characterization of Slurries", investigated the use of Swept-Frequency Acoustic Interferometry (SFAI), which was used for all measurements. SFAI is a frequency-domain technique that transmits a frequency sweep signal into the container of interest with a receiver on the opposite side of the container to measure the frequency response of both the container and the liquid held within. Based on the elastic properties of the liquid within, standing waves (resonances) will be set up in the system. Sound speed can be calculated by determining the frequency difference between two successive resonances, while sound attenuation is obtained from additional signal processing in the inverse space, through the FFT (Fast Fourier Transform) peak ratio. Figure 24 shows an example of the input signal at the top as well as a typical received signal on the bottom.

Two different types of surrogates were used in these studies, along with calibration measurements on liquids with well-known elastic properties. The two types of surrogates were provided to us by NEN-1 (Nuclear Engineering & Nonproliferation), Hanford HLW Simulant, and FIU (Florida International University), Kaolin.

Pure water

Initial calibration was performed using high purity HPLC (High-Performance Liquid Chromatography) water. Standard equipment (Anton Paar DSA 5000M) was used to calibrate data for sound speed, sound absorption/attenuation and density.

In the next step, a specialized SFAI cell was built, such that we can get accurate measurements of elastic properties of liquids. The cell consists of high purity quartz glass and can be used at later stages either for calibration of samples on-site, and/or for sampling purposes in the field, leading to accurate measurements. Additionally, we developed a new data analysis approach that provides very accurate measurements, in great agreement with theoretical/standard values, see Figure 24. Several improvements were made in signal processing to obtain more accurate values for the quantities of interest. The experimental data basically overlap with both theoretical and calibration data from Anton Paar.

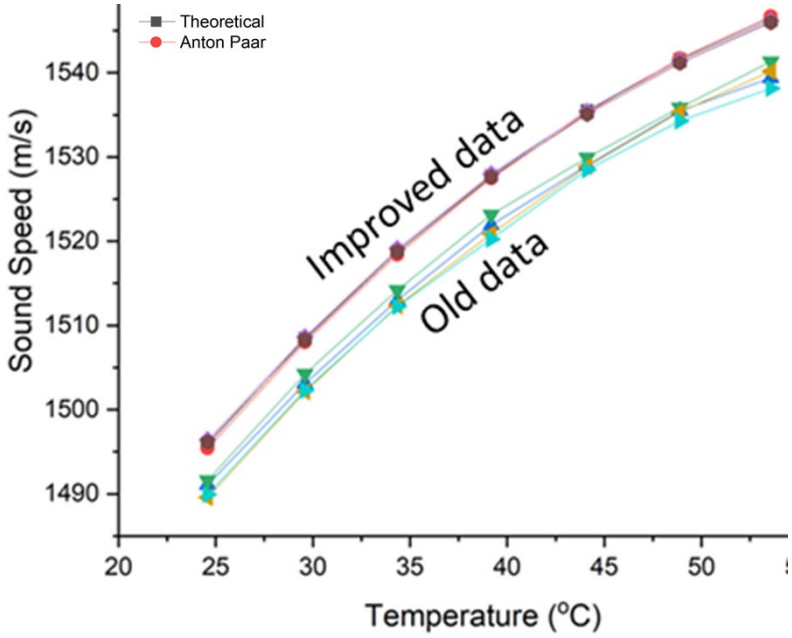

Figure 24 - Sound speed data obtained from SFAI measurements in a glass Starna cell.

Hanford HLW Simulant

Seven different Hanford HLW simulants were obtained from the LANL LIBS team. They consist of different concentrations of chemicals specific to the Hanford site. Recipes are available upon request. Sound speed and density were measured first, for calibration purposes, using an Anton Paar instrument. Data are summarized in Figure 25.

Next, we performed sound speed measurements of three simulant solutions with different concentrations: EMF-1, EMF-3 and EMF-15 in the SFAI cell. A short summary is provided in Table 1 below. Data from the SFAI cell is in good agreement with the calibration data. The main conclusion that can be drawn from these measurements is that samples EMF-1 and EMF-3 are identical from the point of view of elastic properties determined here.

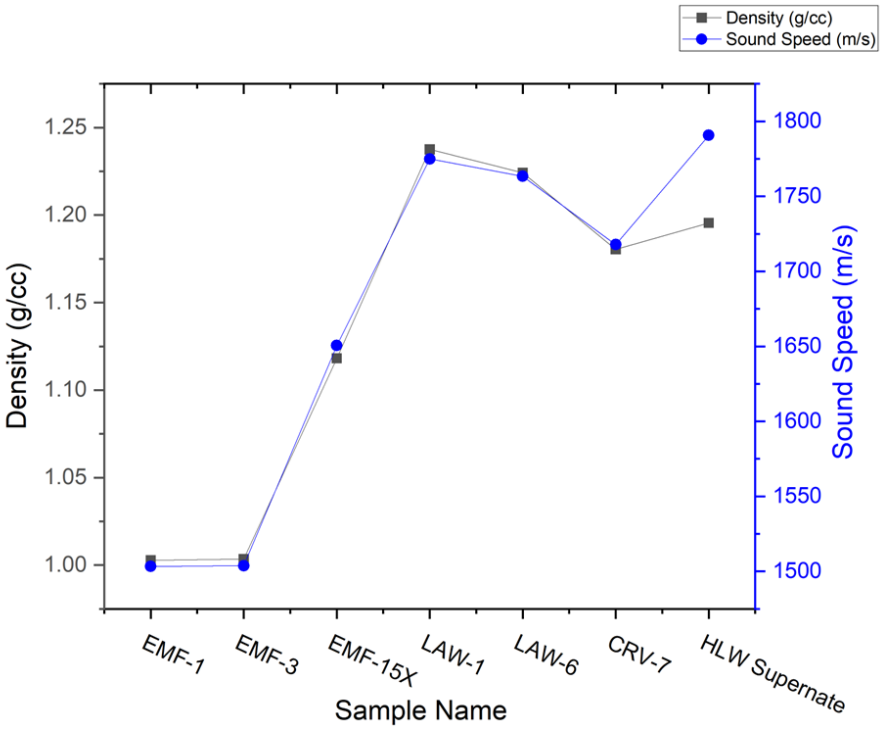

Figure 25 - Sound speed and density for seven different Hanford HLW simulants.

Table 1. Recipes for three of the Hanford HLW simulants.

Concentration (g/L)	EMF-1	EMF-3	EMF-15
$NaNO_3$	0.0608		
NaCl	1.916	1.553	28.29
NH_4NO_3	4.6946	4.6703	66.12
NH_4Cl		0.2629	
Na_2SO_4	1.1585	1.9241	11.841
NaF	0.2664	0.1647	3.531
KF	0.414	0.558	2.721
Na_2CrO_4	0.081	0.081	0.912
$NaAlO_2$	0.0164	0.0164	0.18
$Na_2HPO_4{\cdot}2H_2O$	0.0314	0.0314	0.317
HCl	0.617	0.617	6.965
$Se(NO_3)_6$	0.0203	0.0203	
$Hg(NO_3)_2$	0.0052	0.0052	
$As(NO_3)_5$	0.0119	0.0119	
$Sb(NO_3)_5$	0.0073	0.0073	
$Pb(NO_3)_2$	0.001	0.001	
NaOH			120.09

Kaolin

Kaolin was used as a surrogate to be shared between sites as a standard and was shipped from FIU to all participants. Kaolin solutions with different concentrations were prepared, with concentrations ranging from 0% to 30%, in increments of 5%, Figure 26(a). The Kaolin settles relatively quickly, and a magnetic stirrer was used for keeping the suspensions uniformly in the liquid, Figure 26(b).

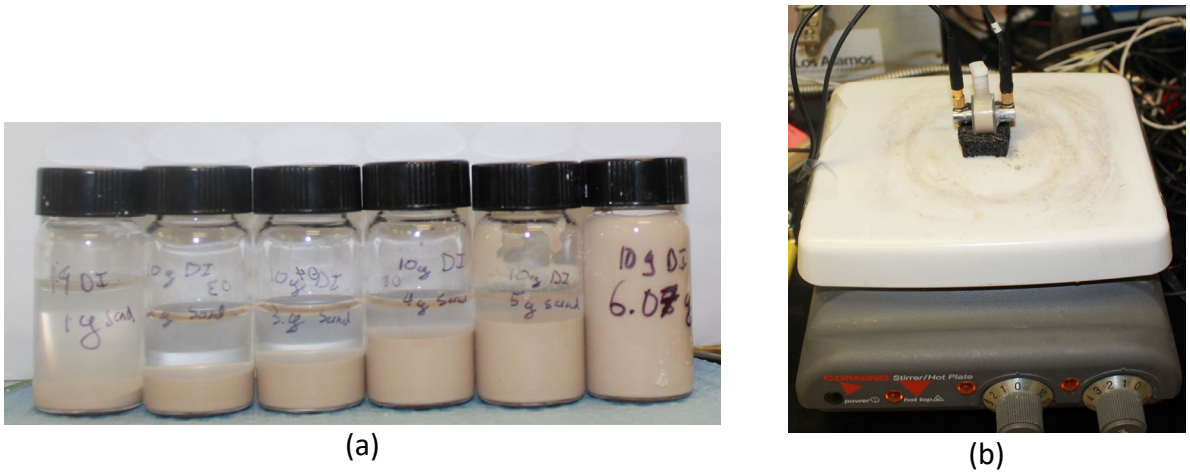

(a) (b)

Figure 26 - Kaolin simulants of different concentrations. (a) Left, settled, and (b) right, in a Starna cell, with magnetic stirrer.

Sound speed dependence with Kaolin concentration is shown in Figure 27, while attenuation coefficient vs concentration of Kaolin is shown in Figure 28. Measurements were performed in a controlled temperature environmment, at 25 °C.

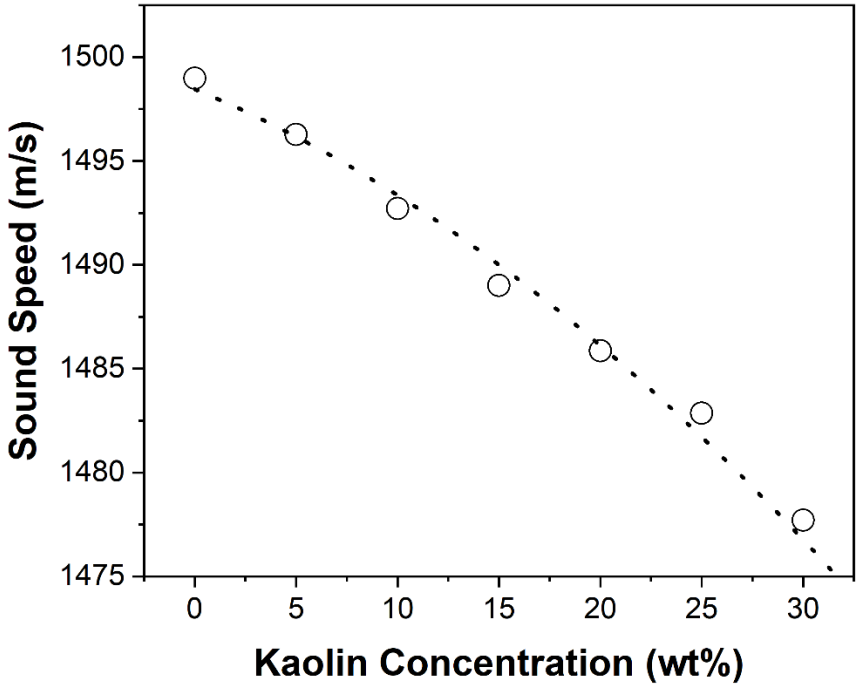

Figure 27 - Sound speed at room temperature vs Kaolin concentration.

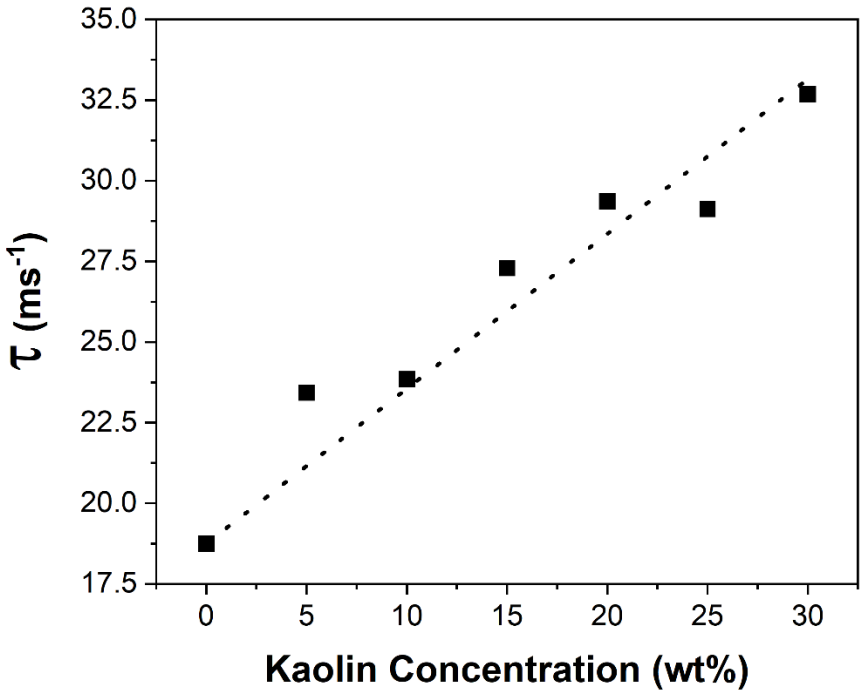

Figure 28 - Sound attenuation coefficient at room temperature vs Kaolin concentration.

Acoustic Conclusions

Signal processing procedures were developed for accurate determination of elastic properties of liquids of interest. Specifically, sound speed and attenuation coefficient were determined from SFAI spectra obtained from a liquid in a sampling cell (Starna cell).

Sound speed measurements derived from SFAI spectra are in good agreement with book values, and also with experimental values determined with an Anton-Paar meter.

Calibration curves were obtained for Kaolin, a surrogate that will be used between different sites involved in the project. The quantities of interest are (1) sound speed, and (2) sound attenuation coefficient.

Flow Loop and integrated diagnostics

High-level radioactive waste at Department of Energy complex sites often takes the form of non-Newtonian slurries that pose significant challenges for safe, efficient transfer through piping networks. To address these challenges, FIU is investigating an in-line monitoring system designed to characterize non-Newtonian slurry behavior under realistic flow conditions. Our primary focus lies in real-time measurement of flow rate, density and pressure to determine the yield stress, which is a critical parameter that can govern operational efficiency and safety margins. Figure 29 below demonstrates flow characteristics of various fluid types as they relate to shear stress and strain.

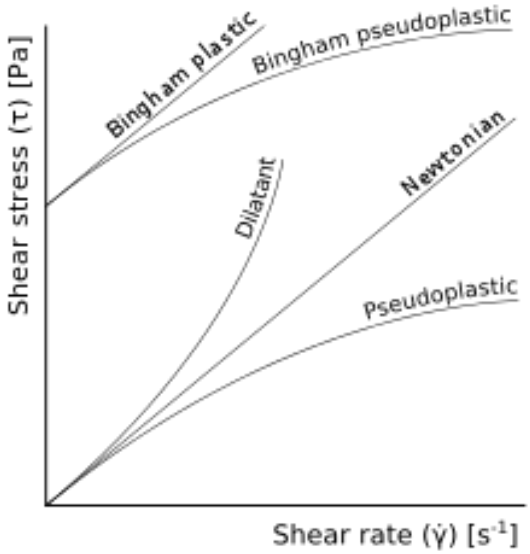

Figure 29 - Shear curves for various fluid types

The yield stress of a fluid can increase the size of equipment needed to transport or mix the slurries and can increase the risk of process upsets[iv]. Current methods of sampling include manual sample collection and transportation to a laboratory. This process can increase risk of personnel exposure to radiation and increase secondary waste. It also delays results and the slurry rheological properties may change during the sampling and transport to the laboratory.

Previous work by FIU funded under DOE–EM's MSIPP program demonstrated potential yield stress monitoring methods using a 1-inch diameter loop with kaolin/water slurries. Approaches included using a liquid rise method and a pressure loss method. The figures below show the loop set up and results from the two approaches.[v, vi]

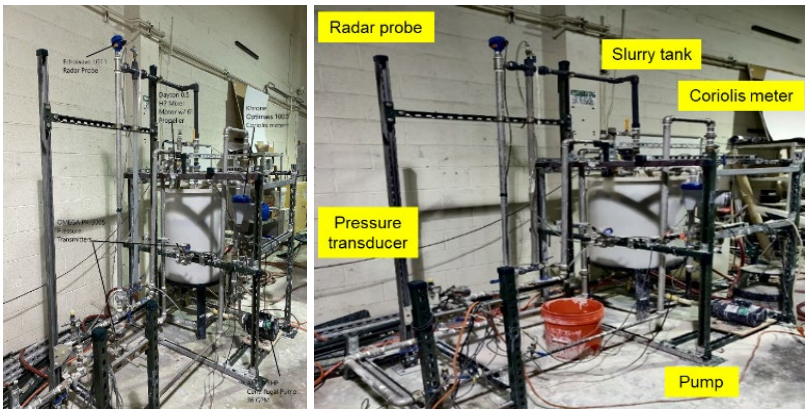

Figure 30 - 1-inch diameter flow loop for determining yield stress of slurry.

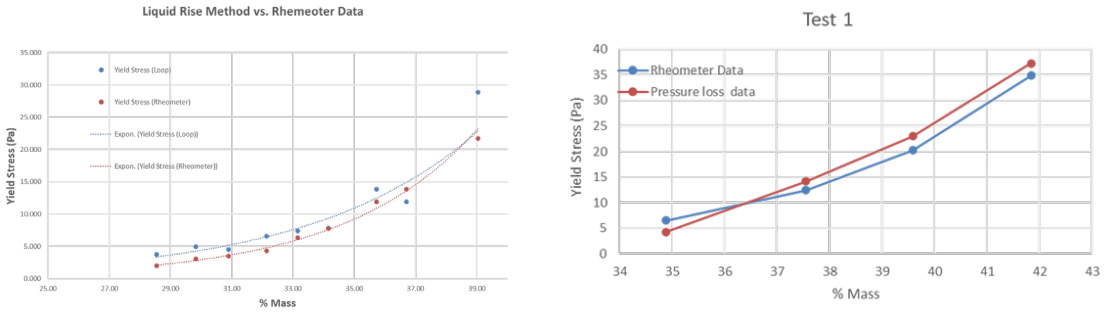

Figure 31 - Yield stress measurements using the liquid rise and press lose methods.

Objectives

The proposed objectives in this research effort for FIU include the following:

- Develop a larger scale loop, 2-inch and 3-inch in diameter, and evaluate accuracy of yield stress measurements, as the system is scaled up with kaolin/water slurry.
- Utilize additional simulants more representative of the waste and evaluate ability to obtain reliable and repeatable yield stress measurements.
- Work with team members to integrate other RTIM methods into our engineering scale loop and ultimately conduct a demonstration of the proposed techniques using the loop at FIU.

Technical Progress

A closed-loop, two-inch-diameter steel pipe testbed is being constructed to circulate kaolin–water slurry at varying weight percentages of kaolin. This approach enables controlled manipulation of slurry consistency, allowing systematic evaluation of flow properties under diverse rheological conditions. The experimental setup integrates multiple sensor technologies, including a pressure transducer, Coriolis meter, and radar probe, to provide complementary data streams. The pressure transducer offers insights into the local and global pressure variations along the loop, while the Coriolis meter provides accurate measurements of mass flow rate and density changes. Additionally, the radar probe furnishes continuous monitoring of slurry height in the vertical section of the loop, enabling detection of slurry rise in an upright pipe. To capture the essential non-Newtonian characteristics, we will systematically measure yield stress as a function of kaolin concentration and correlate it with observed flow rate and temperature fluctuations. Pressure drop, flow rate, and density measurements show how the yield stress can be characterized in real-time with the changes in slurry composition and how this affects the overall flow stability. Notably, increased kaolin loading exhibits a marked effect on yield stress, underscoring the need for real-time adaptation of pump speed and operational strategies to prevent line plugging.

The pressure loss method utilizes equation (1) for the friction factor and includes the Reynolds number[1] and the Hedstrom number[2], which is a function of the yield stress[vii].

[1] Reynold's Number: a number characteristic of the flow, turbulent or laminar, of a fluid in a pipe or past an obstruction.
[2] Hedstrom number: the ratio of the Bingham Reynold's number, for a Bingham plastic fluid, to the yield stress that gives information on the flow of slurries.

$$f_L = \frac{64}{Re} + \frac{64}{Re}\left(\frac{He}{6.2218Re}\right)^{0.958} \quad (1)$$

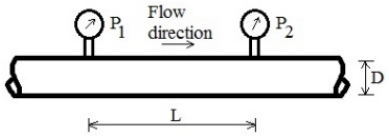

Figure 32 - Pressure loss schematic.

The liquid rise method utilizes the equation (2) to estimate the yield stress[vi]. Two sets of pressure differences are required to solve the unknown yield stress τ_y.

$$\Delta P\left(\frac{\pi(D_2)^2}{4}\right) = \tau_y(\pi D_2 H) + \rho g H\left(\frac{\pi(D_2)^2}{4}\right) \quad (2)$$

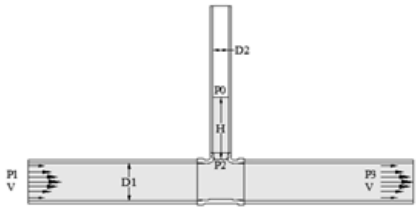

Figure 33 - Liquid rise schematic.

The initial design of the loop incorporates the two methods noted above to obtain yield stress measurements for non-Newtonian fluid is provided in the figure below. This loop consists of 2-inch diameter piping and includes a mixing tank, pump, Coriolis meter, pressure sensors and a radar transmitter. The pressure sensors will provide the pressure loss over a defined distance (5 ft in the figure below) that can be used to estimate the yield stress. Additionally, to improve accuracy of the estimate, fully developed flow is needed so a pipe lead in length proportional to the pipe diameter is needed. The liquid rise method is also incorporated in the loop that involves measuring the height in the flow which can be related to non-Newtonian yield stress in a vertical column. A radar probe is used to measure this height. The Coriolis meter will be used to provide density and flow rates needed for the estimates.

During this performance period, items needed for the development of the loop have been procured. This includes over 40 ft of 2-inch diameter schedule 40 pipe, unions, tees, etc., needed for the loop. In terms of equipment and instrumentation, a mixing tank, mixer and a 2-inch diameter Coriolis meter (Optimass 1000), pressure transducers (PX 3005) and radar probe (LG10-0003-01-072) have been obtained. A National Instruments data acquisition system has also been procured (USB-6451) which has 16 channels for data collection and can be utilized outside, exposed to elevated heat and temperature. The pump is a 10 Hp AMT Centrifugal pump (4250-95) capable of 330 GPM. A VFD (variable frequency drive) was also procured that that variable flow rates can be achieved. For the initial set up and

validation of the pressure loss and liquid rise methods, water/kaolin will be used as the simulant. Thus, enough kaolin has been acquired for both 2 and 3-inch diameter loop testing (20 - 50 lb. bags).

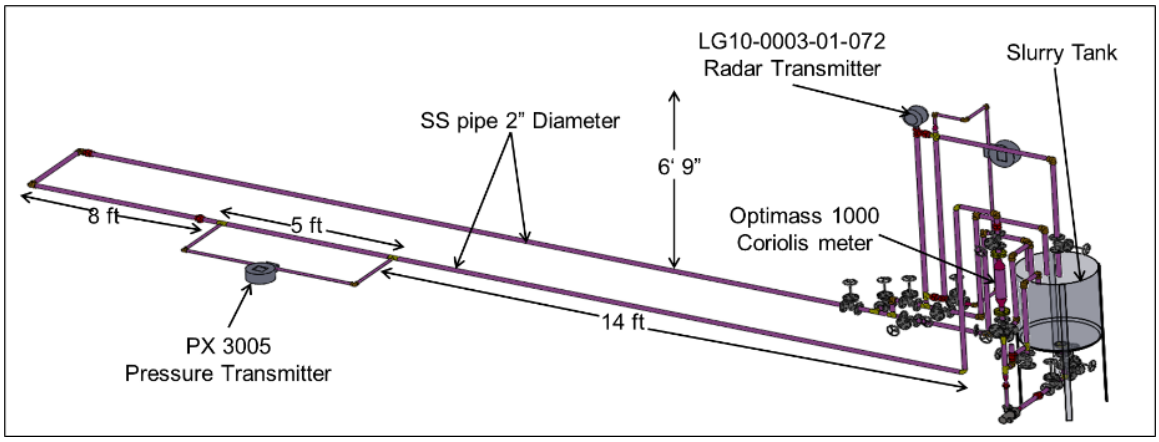

Figure 34 - Yield stress measurements using the liquid rise and press lose methods.

One of the primary accomplishments during this performance period has been the development of the flow loop. Figures of different stages in the loop development are provided below in Figure 35. Due to the length of the loop, it is being constructed outside in a secure area under a 10-ft overhang. Thus, the equipment and sensors will need to be capable of handling the outside environment.

Figure 35 - Flow loop development.

The figure shows the major components of the 2-inch loop have been installed, including the Coriolis meter, pump and tank. The main line has been initially leak tested with minor leaks noted in the connections with the vertical Coriolis meter. These issues have recently been resolved.

In an effort to demonstrate our RTIM system in a realistic setup, our RTIM team has been working with engineers from Hanford to discuss options regarding where the system could potentially be deployed. The idea would be to incorporate constraints into our flow loop similar to what would be encountered for deployment in the field. The discussions have led to a few options including potentially deploying the system into a tank pit similar to pit 241-AP-05A. This particular pit is approximately 14'x18'x5' and receives three tank risers. It includes a 2-inch diameter slurry line and a 3-inch supernate line. For demonstration purposes, the RTIM system could be installed in the pit with the waste being recirculated back into the tank. In addition, it would be possible to implement either a 1-inch or 2-inch diameter slip stream off of the two lines in the pit and incorporate the RTIM system prior to feeding the waste back to the line or recirculating back into the tank. In Figure 36, a 1-inch diameter slip stream is pulled off of the

2-inch slurry line and returned back to the line. The concept is to integrate the analytical tools and sensors proposed for our RTIM system on the slip stream, providing rheological and chemical information real time without disruption in the transfer.

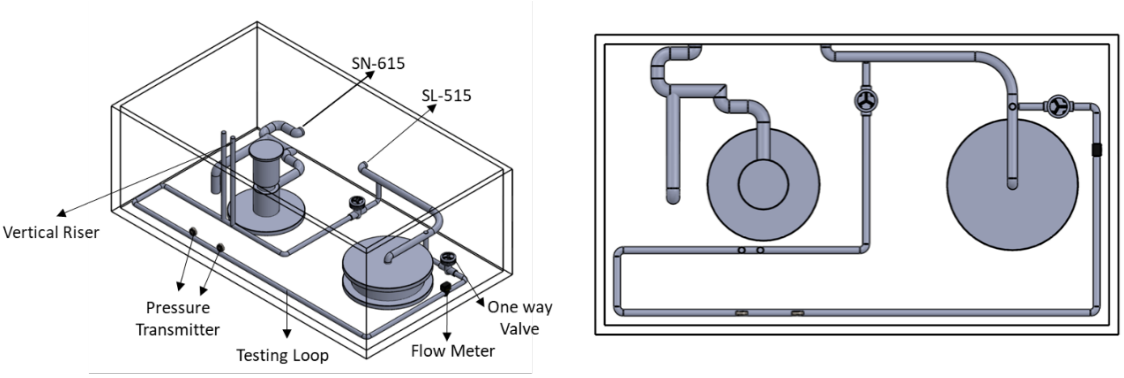

Figure 36 - Potential slip stream lines and locations for pressure loss and liquid rise system.

Path Forward

In the next performance period, the RTIM Team will continue to work with engineers at Hanford to solidify our approach for deployment. Once the deployed approach is agreed upon, the flow loop will likely be augmented to include both 1 and 2-inch diameter loop sections. The various challenges associated with implementation of the yield stress sensors will be addressed and integrated into the flow loop. This will include the variable flow rates and pipe length needed for the pressure loss method and the height and close loop requirements needed for the liquid rise method. Yield stress measurements will then be conducted with a kaolin/water simulant at various concentrations of kaolin. Efforts will then focus on modifying the loop to integrate the analytical chemistry tools (LIBS, FTIR, and Raman Spectroscopy) and acoustic sensors. More realistic simulants will also be utilized, which will likely require safety modifications to the loop and a chemical pump. Integration of the analytical chemistry tools could require alternate means to control the flow rate. In addition, we will likely incorporate a means to elevate the temperature of the loop, to emulate temperatures typically seen in the tanks (up to 160 F).

Waste Form Synthesis

Waste Stream Analysis

An important element of the development and demonstration of technology for real-time monitoring of high-level waste (HLW) slurry is an understanding of the likely composition and properties of the sample streams that will be analyzed. The starting point for achieving this understanding is knowing what is stored in the HLW tanks. Waste processing will be done in a considered manner, as material brought to the Hanford vitrification facilities is limited by waste acceptance criteria (WAC) to protect safety and process control limits (PCL) to ensure waste glass quality. The contents of HLW storage tanks vary substantially due to the different processing campaigns over the history of the Hanford site. Also, within a given tank, as the contents have not been routinely agitated, material has separated into distinct layers with different chemical and physical properties. Many of these individual layers have properties

that do not meet WAC and PCL requirements. Thus, individual processing campaigns will be conducted to blend layers from different tanks to achieve slurry streams that meet safety and quality metrics. Real-time monitoring will help ensure that this blending is having the desired effect.

Prior work has generated estimates of the layer blending required for processing campaigns to meet WAC and PCL requirements[viii]. This work describes a series of campaigns that can be constructed to process all of the waste in the tanks under these requirements. In some campaigns, the predicted levels of certain species closely approach their relevant WAC and PCLs. These calculations do not include any uncertainties associated with the concentrations. It is likely that there are appreciable uncertainties associated with analytical measurements of retrieved tank waste samples, the representativeness of the retrieved samples (i.e. homogeneity of the layers), and the quantity of the layers being retrieved. Real-time monitoring of sampled tank layers and/or materials in a blending tank will help ensure that WAC and PCLs are being met during the blending process and support any adjustment made to the material before it is brought to the processing facility.

The calculational analysis reported here addresses several key aspects of the development and eventual deployment of real-time monitoring technology. As discussed above, some material concentrations are at risk of exceeding their limits. This analysis identifies these at-risk properties, generating a prioritized analyte list that can be a focus of subsequent instrument development. Relatedly, the expected concentrations of the analytes can be established, informing the construction of test simulants as well as providing appropriate targets for method sensitivities. Where the analysis specifies certain analytes to be of high importance but at low concentrations, suitable higher-concentration marker species may be identified. These marker species would have concentrations that are correlated (across multiple layers) with the actual species of interest but are easier to measure accurately. The analysis also tracks the distribution of species between the solid and supernate phases of the slurry. Spectroscopy-based chemical analysis methods are often dependent on the form of the analyte or the entire material. A comprehensive understanding of the expected phases of the material will drive appropriate method development and validation.

Key Resources

Key data resources used in this work include two primary workbooks, both associated with Retrieved Waste Stream Composition (RWSC)-145: *RPP-RPT-64878_01, App D, Layer-By-Layer Feed Vector and Analysis.xlsx* and *RPP-RPT-64878_01, App E, Blended Feed Vector and Analysis.xlsx.* Both workbooks contain information on analytical constituent amounts for a given tank waste layer or blended feed vector, the associated slurry stream properties (e.g. volume, mass, density), and calculated WAC and PCL values. Detailed descriptions of these workbooks and their contents can be found in the appendices of Direct-Feed High-Level Waste Feed Vectors Assessment[viii]. This document also provides a list of the WAC and PCL criteria and limits. As indicated in the filenames, the first workbook contains data associated with each tank waste layer to be blended, while the second presents data associated with potential blend campaigns including fractional amounts of each waste layer to be blended. In both workbooks, all values are presented for different feed vector scenarios representing varying levels of the following parameters: (1) the supernatant density used to support tank solids retrieval, (2) the target liquid density, and (3) the target solids loading, where the latter two are achieved through the addition of a secondary liquid effluent. The analyses presented here focus on the scenario with a target supernatant density of 13.5 g/mL, slurry liquid density of 12 mg/L, and solids loading of 20 wt.% (labeled

Feed_125.120.200 and BFeed_135.120.200 in the workbooks listed above, respectively). This scenario was selected as representative of a challenging case for real-time monitoring methods, namely the 20 wt.% solids loading. The loading level was chosen due to a likely preference for higher solids loading values to reduce the volume of material being processed and amount of water being removed during vitrification.

At-Risk Analytes via Monte Carlo Simulation

To identify at-risk analytes in the given feed vector scenario, Monte Carlo (MC) simulations were applied to simulate the effects of uncertainties that exist in the reported analyte concentrations, which may result from several sources. The analytical measurement techniques used to derive the reported concentrations values naturally contribute to uncertainty, though the magnitude of this effect for each analyte is currently unknown. Further, the sample aliquots of each layer analyzed may not be fully representative of the entire layer due to potential heterogeneity. Similarly, the waste layers represented in this data are non-discrete, meaning that any mixing that may occur at layer interfaces is not represented in the reported analyte concentrations. Finally, when considering the transfer of waste for blending, there is likely some error in the total amount of waste being blended from each layer, leading to further uncertainty in the final concentrations reported for potential blended feed vectors.

To better understand which analytes are at risk of exceeding the WAC and PCLs, a 20% error was incorporated into each analyte at the waste layer level and propagated via MC simulation to generate concentration ranges for WAC and PCL values of each blend campaign. This singular error level was selected in lieu of access to any reported uncertainties for each analyte concentration. Based on the propagated uncertainty, analytes that exceeded 80% of, or surpassed, the WAC or PCL were recorded and categorized as at-risk analytes for each of the 17 blend campaigns. The results are summarized in Table *2*. An example of the WAC/PCL values including estimated uncertainty for blend Campaign 3[3] is presented in Figure 38. Similar analysis was performed for each of the 17 campaigns. Results are plotted as fractional values of the WAC or PCL so that all parameters can be displayed alongside one another. Certain parameters that would not be addressed using the real-time analysis methods being considered in this project (e.g. unit dose, equivalent Cs-137 concentration, etc.) are not included in the displayed analysis. Also, the solids loading, bulk density, and liquid density parameters all exceed 80% of the WAC since these are pre-defined values of the feed vector scenario selected (i.e. Feed_135.120.200).

The results indicate that the chemical WAC/PCLs that are the most significant targets for real time measurements are the sum of nitrate and nitrite concentrations, the weighted sum of Na and K concentrations ([Na] + 0.59[K]), the sum of Al, Fe, and Zr concentrations, and sulfur. Additionally, thorium levels are potentially high for one campaign.

[3] Campaign 3 is a blend of four layers with origins as follows: 37% of AN-103 Layer 1, 100% of AW-101 Layer 1, 49% of AW-104 Layer 1, and 10% of AW-106 Layer 1.

Table 2. Summary of analytes exceeding margin and surpassing WAC/PCL for the 17 campaigns.

WAC/PCL	Times Exceeding 80% Margin	Time Exceeding WAC/PCL	Total
$[No_x^-]^a$	1	6	7
NaK[b]	3	11	14
AlFeZr[c]	3	5	8
S	9	0	9
Th	1	0	1

[a] $[No_x^-] = [NO_2] + [NO_3]$
[b] NaK = [Na] + 0.59[K]
[c] AlFeZr = [Al] + [Fe] + [Zr]

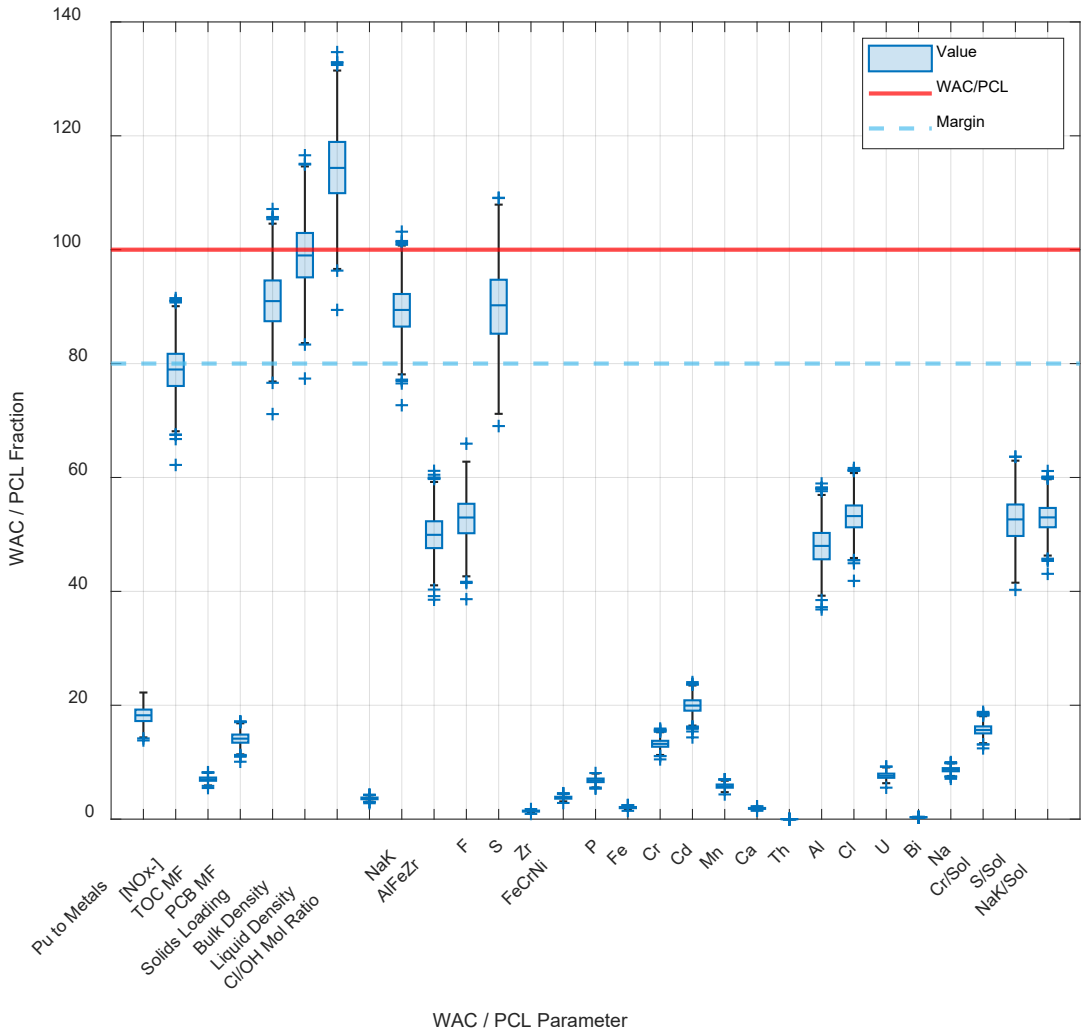

Figure 37 - Distribution of WAC/PCL fractional values resulting from MC simulation of campaign 3.

Concentration Levels of At-Risk Analytes

For those analytes (or groups) that are identified as at-risk and that are most compatible with the real-time methods under investigation, the average concentration across waste layers and campaigns was investigated further (Figure 39). This information will be useful for comparison against the analytical detection limits of these methods as well as to support development of realistic simulants for method development.

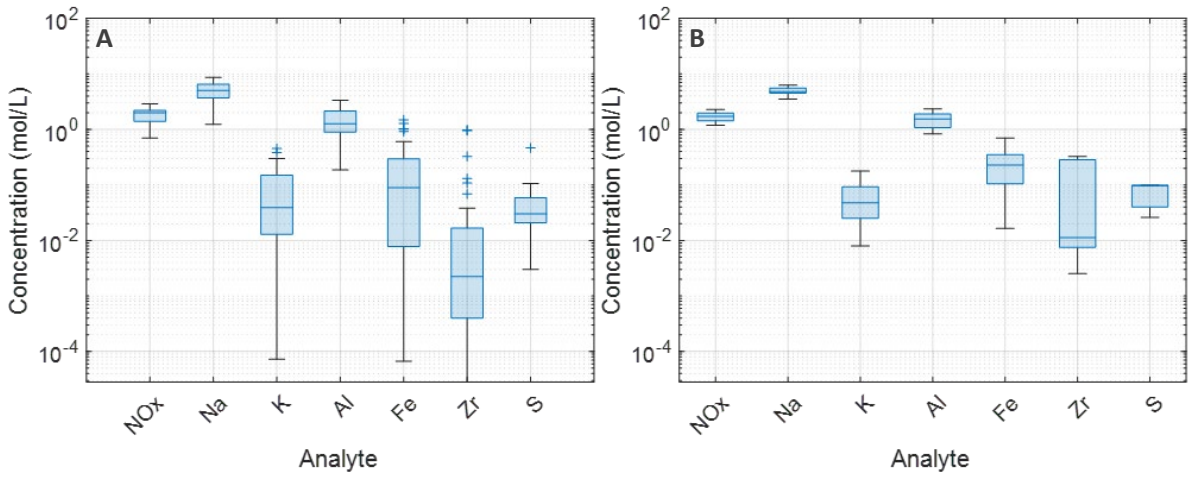

Figure 38 - Analyte concentration ranges for (A) waste layers and (B) blend campaigns

The efficacy of the blending calculations can be observed through the narrower distribution of concentrations across campaigns (Figure 38b) compared to the individual layers (Figure 38a). All of the analytes shown except sulfur are present with concentrations that are anticipated to be well above the detection limits of the methods being tested, even with the added complication of the two-phase composition of the slurries.

Future Work

In addition to the total concentration of the analytes identified, it is also necessary to understand the distribution of these analytes across the solid and liquid phases. Ongoing work is being conducted to ascertain the solid/liquid fractions and concentrations for the at-risk analytes of interest identified. Preliminary results (obtained by the end of the first year) suggest that NO_x will be mainly in the supernate, Fe and Zr predominantly in the solid phase, and Na, K, and Al in a campaign-dependent distribution between the two phases. The results for Na, K, and Al highlight the need to evaluate the ability of instrumental methods to measure species in both phases without bias. Work on the distribution of S also seems to indicate that it will be present in two phases – sulfate ion in the supernate, and supersaturated kogarkoite (Na_3FSO_4) in the solids. Both elemental (LIBS) and molecular (Raman, ATR-FTIR) methods are possibly relevant for detection of these species.

Future work will also focus on determining if marker species exist for S, whose concentration may be near or below detection limits of the real-time monitoring methods. It is anticipated that the potential marker species required may vary by waste campaign. Marker species will be identified by a demonstrated correlation between the species across all layers that comprise a campaign.

Simulant Preparation

A proper slurry simulant for testing real-time analytical measurement technologies should have several characteristics. It should represent as closely as possible the chemical and physical properties of HLW slurries without introducing unnecessary issues associated with disposal (i.e. no RCRA metals) or radioactivity. Distributions of analytes between solid and liquid phases should mimic actual slurries, so that the analytical techniques being studied are tested appropriately. It should be modular, allowing different laboratories to tailor solids loading content. It should be alterable so that calibration curves can be developed for the analytes. And ideally, it should be comparatively inexpensive and easy to prepare. The latter point is relevant to the use of test loops as is planned for later years of this project. A 2" diameter test loop could require 15-20 gallons of simulant to run properly.

Simulant selection

A number of simulants have been prepared at SRNL and PNNL over several decades to represent slurries, glass forming chemicals, and other materials used in vitrification. A noteworthy example is a simulant developed for the Pretreatment Engineering Platform (PEP) test bed.[4] This simulant has six components, which are described in Table 3. These components are further described below. The simulant is formulated so that the solids and supernate can be separately formulated and added together as needed to achieve a desired solids loading.

Table 3. Summary of components in PEP simulant and use for analytical simulant.

Component	Description	How used	Proportion (wt.%)[a]
Boehmite	Solid	Included	95.0
Gibbsite	Solid	Included	1.78
Oxalate	Na oxalate (dissolved)	Included	1.78
Filtration	Also called "Fe-rich sludge simulant". Contains solids and is shimmed with supernate (below)	Modified	0.515
Supernate	Also called "specific supernate"	Included	0.935
Chromate	CrO(OH)	Omitted	0

(a) Recipe for a 5-wt% undissolved solids PEP simulant (would be proportionally modified for a 20-wt% simulant for analytical work).

Boehmite and gibbsite. In the original PEP simulant, boehmite (AlO(OH)) and gibbsite ($Al(OH)_3$) were commercially sourced.[5] The materials were selected based on the similarity of their morphological properties (crystal size, shape) to those of solids observed in tank waste samples.[6] Unfortunately, both commercial products have been discontinued by their manufacturers. Other grades of these materials

[4] R.D. Scheele, G.N. Brown, D.E. Kurath. "Scale-up, Production, and Procurement of PEP Simulant". PNNL-18678, WTP-RPT-204, Rev. 0. PNNL, October 2009 (and references therein).
[5] Boehmite: Nabaltec Apyral OH 20. Gibbsite: Almatis C333.
[6] H.D. Smith, R.L. Russell, R.A. Peterson, "Simulated Waste for Leaching and Filtration Studies – Laboratory Preparation Procedure". PNNL-18701, WTP-RPT-201, Rev. 0. PNNL, October 2009.

are available and are being evaluated to determine which one will be the most suitable for the analytical simulants.

Oxalate. Commercially available sodium oxalate is dissolved as part of the preparation procedure. This material is readily available.

Filtration solids. Also known as "Fe-rich sludge simulant", this solids-heavy material is prepared by dissolution of metal nitrate salts, precipitation of the metals as oxides, and shimming with a representative supernate simulant to match the liquid phase composition. Expected concentrations of these components from batches prepared in the original PEP simulant are shown in Table 4. This material is modified so as to remove any RCRA-listed metals.

Table 4. Expected Filtration Inerts Composition for PEP Simulant.

Constituent	Concentration (μg/g)	Constituent	Concentration (μg/g)
Al	0	Mn	98,500
Ca	13,400	Nd	11,200
Ce	5,440	Ni	15,000
Fe	460,000	Sr	3,720
La	4,010	Zr	12,100
Mg	4,210		

With respect to the tank waste analysis provided in the previous section, this filtration simulant provides the Fe and Zr expected in the solids phase at 40x different concentrations. This material would be a suitable test for the LIBS technique for the measurement of bulk (Fe) and low/intermediate (Zr) metals in the solid phase of a slurry. Note that solid-phase Al is provided by the boehmite and gibbsite. All chemicals used to prepare this material are readily commercially available.

Supernate. Table 4 provides the expected concentrations of elemental and molecular species in the solution phase of the slurry. The expected density of the supernate is 1.23 g/mL. This liquid contains substantial amounts of Na, NO_2^-, NO_3^-, and S (as SO_4^{2-}) as well as a small amount of Al.

Table 5. Expected concentrations in supernate.

Constituent	Concentration (μg/mL)	Constituent	Concentration (μg/mL)
Al	3,370	NO_3	99,100
Na	115,000	PO_4	6,250
P	2,040	SO_4	16,900
S	5,640	TIC	6,640
C_2O_4	1,250	TOC	341
NO_2	23,300	OH	18,500

Chromium. Chromium is not an analytically important component with respect to the protection of WAC/PCLs. Therefore, we have chosen a recipe that omits this material.

Future work

In Year 2, SRNL will take the following steps leading to distribution of the solid and supernate components to the partner labs.

- Identify suitable replacement sources of boehmite and gibbsite. Note that previous work with Raman and ATR-FTIR spectroscopies has shown some dependence on both overall solids signal and attenuation of signal from liquid-phase analytes to be dependent on the morphology of the solids.[7]
- Consider adjustments to the recipe to reflect findings from the tank waste analyses. For example, where there may be a distribution of S between the solid and supernate, addition of kogarkoite (the source of S found in the solids) may be indicated. However, it remains to be seen if the kogarkoite will be supersaturated (and remain in the solid phase) in real slurries.
- Procure any other needed chemicals and make the two components.

We will initially make smaller batches (~ 1 L) that will suffice for laboratory-scale studies. Larger batches suitable for test loop use will be made at a later date.

Year 1 Tasks and Milestone Progress

WBS	Task Name	% Complete	Start	Finish
	RTIM Gant Chart Y1	37%	Mon 4/15/24	Sun 2/28/27
1	**CRESP/Georgia Tech**	**95%**	**Wed 5/1/24**	**Mon 6/30/25**
1.1	Design calibration data set for slurry measurements.	100%	Wed 5/1/24	Sun 6/30/24
1.2	Complete IR and Raman measurements on the calibration data set.	100%	Mon 7/1/24	Fri 8/30/24
1.3	Design and test algorithms and code for sensor fusion.	100%	Thu 8/1/24	Mon 9/30/24
1.4	Analyze data for composition estimation	100%	Tue 10/1/24	Sat 11/30/24
1.5	Prepare and submit publication on data fusion in slurry	85%	Sun 12/1/24	Mon 6/30/25
1.6	Collect data on fouling of IR probe	100%	Wed 1/1/25	Fri 2/28/25
1.7	Analyze fouling data and develop software models to eliminate its effect on estimation	100%	Sat 3/1/25	Wed 4/30/25
2	**SRNL/FIU Subcontract**	**42%**	**Wed 5/1/24**	**Mon 9/1/25**
2.1	HLW tank data meta-analysis	95%	Wed 5/1/24	Mon 9/30/24
2.2	LLW tank data meta-analysis	0%	Tue 10/1/24	Mon 9/1/25
2.3	Prepare/submit publication on tank data	0%	Tue 4/1/25	Mon 6/30/25
2.4	Design simulants	100%	Wed 1/1/25	Sat 2/15/25

[7] R.J. Lascola and M.E. Stone, "Real-Time, In-Line Monitoring for High Level Waste Applications". SRNL-RP-2023-01064, Rev. 1. SRNL, September 2024.

2.5	Make simulants	2%	Sun 2/16/25	Fri 8/1/25
2.6	Procure ReactIR probe	100%	Mon 7/1/24	Thu 8/15/24
2.7	Probe irradiation testing	75%	Fri 8/16/24	Fri 8/1/25
3	**Development of Enhanced LIBS Techniques**	**33%**	**Mon 4/15/24**	**Thu 12/31/26**
3.1	LIBS: Sampling Method Development (for liquids and slurries)	50%	Mon 4/15/24	Wed 9/30/26
3.2	LIBS: Equipment design and acquisition.	15%	Mon 7/1/24	Tue 9/30/25
3.3	LIBS: Enhancing Analytical Sensitivity	60%	Mon 3/31/25	Wed 9/30/26
3.4	LIBS: Method development and testing.	25%	Wed 1/1/25	Thu 12/31/26
3.5	Numerical Method Development	30%	Mon 7/1/24	Thu 12/31/26
3.6	Calibration Optimization	25%	Mon 7/1/24	Thu 12/31/26
3.7	Analytical results classification	25%	Mon 7/1/24	Thu 12/31/26
4	**LANL Acoustic Characterization of Slurries**	**34%**	**Wed 5/1/24**	**Sun 2/28/27**
4.1	Measurement of Acoustic Properties	95%	Wed 5/1/24	Fri 8/1/25
4.2	Flow-Loop Testing	10%	Thu 5/1/25	Fri 7/31/26
4.3	LANL FIU Field Trial	0%	Fri 10/24/25	Sun 2/28/27
5	**Flow Loop Testing**	**28%**	**Tue 8/20/24**	**Tue 6/30/26**
5.1	2" Flow Loop Development and Testing	75%	Tue 8/20/24	Wed 7/30/25
5.2	Development of 3-inch Flow Loop	5%	Tue 10/1/24	Tue 9/30/25
5.3	3-inch Flow Loop Testing	0%	Wed 10/1/25	Tue 6/30/26

[i] Crouse, S. H., Rousseau, R. W., & Grover, M. A. (2024). A feature selection method for overlapping peaks in vibrational spectroscopy using nonnegatively constrained classical least squares. *Computers and Chemical Engineering*, *189*(July), 108785. https://doi.org/10.1016/j.compchemeng.2024.108785

[ii] R.J. Lascola and M.E. Stone, SRNL-RP-2023-01064, Rev. 1. “Real-Time, In-Line Monitoring for High Level Waste Applications”. Savannah River National Laboratory, September 2024.

[iii] A.N. Gurzhiev *et al. NIMPR A* **391** (1997) 417-422. “Radiation damage in optical fibers”

[iv] M. Farrar, M. Poirier, C. Herman, C. DiPrete, A. Howe, M. Stone, F. Miera, W. Hamel, I. Wheeler and B. Mauss, "Instrumentation for Hanford Direct-Feed Low Activity Waste Real-Time, In-Line Process Monitoring - 18339," in Waste Management Symposia, Phoenix, AZ, USA, 2018.

[v] B. Cintas, A. Saha, S. Tashakori, M. Poirier, D. McDaniel, “Development of Methods for In-line Monitoring of Yield Stress During the Transfer of Radioactive Waste”, Proceedings of the Waste Management Symposia 2021, Phoenix, AZ, March 7-12, 2021.

[vi] A. Baharanchi, A. Saha, B. Cintas, D. McDaniel, M. Poirier, “Development of Methods for In-line Monitoring of Yield Stress During the Transfer of Radioactive Waste - 20435”, Proceedings of the Waste Management Symposia 2020, Phoenix, AZ, March 8-12, 2020.

[vii] P. K. Swamee, P. N. Rathie and N. Aggarwal, "Exact solution of friction factor and diameter problems involving laminar flow of Bingham plastic fluids," *Journal of Petroleum and Gas Exploration Research,* vol. 2, no. 2, pp. 27-32, 2012.

[viii] M.D. Britton and C.K. Anderson, RPP-RPT-64878, Direct-Feed High-Level Waste Feed Vectors Assessment, Rev 0, June 2024.